A Clasical RING Finger

C-x (2) -C-x (9-39)-C-x(1-3)-H-x(2-3)-C-x(2)-C-x(4-48) Ⓒx(2)Ⓒ

Mel-18 RING Finger

CALCGGYFIDATTIVECLHSFCKTCIVRYLATNKYCPMC

Figure 5. A Mutation in the RING Domain of Mel-18 Abolishes Ubiquitylation of Nucleosomes, but Not Free Histones

(A) Amino acid sequence of a consensus RING domain and the RING domain of Mel-18. Boxed residues represent the amino acids mutated and correspond to the circled residues of the consensus RING domain.

(B) Wild-type and mutant Ring1B/Mel-18 complexes. Molecular weight markers are indicated.

(C) Mutant Ring1B/Mel-18 complexes were examined for ubiquitylation of nucleosomes. I^{125}-ubiquitylated histone H2A (H2Aub1) and autoubiquitylated Ring1B/Mel-18 (asterix) products are indicated.

(D) Mutant Ring1B/Mel-18 complexes were examined for ubiquitylation of individual histones. Reactions were performed using 1 μg of recombinant histones (as indicated). I^{125} autoubiquitylated Ring1B/Mel-18 (asterix) product is indicated.

nucleosomal targeting of melPRC1 requires prior phosphorylation of Mel-18. Collectively, these results show that the RING finger protein Mel-18 plays a critical role in recruiting polycomb proteins to chromatin and provide a link between polycomb-mediated gene repression and cell signaling pathways.
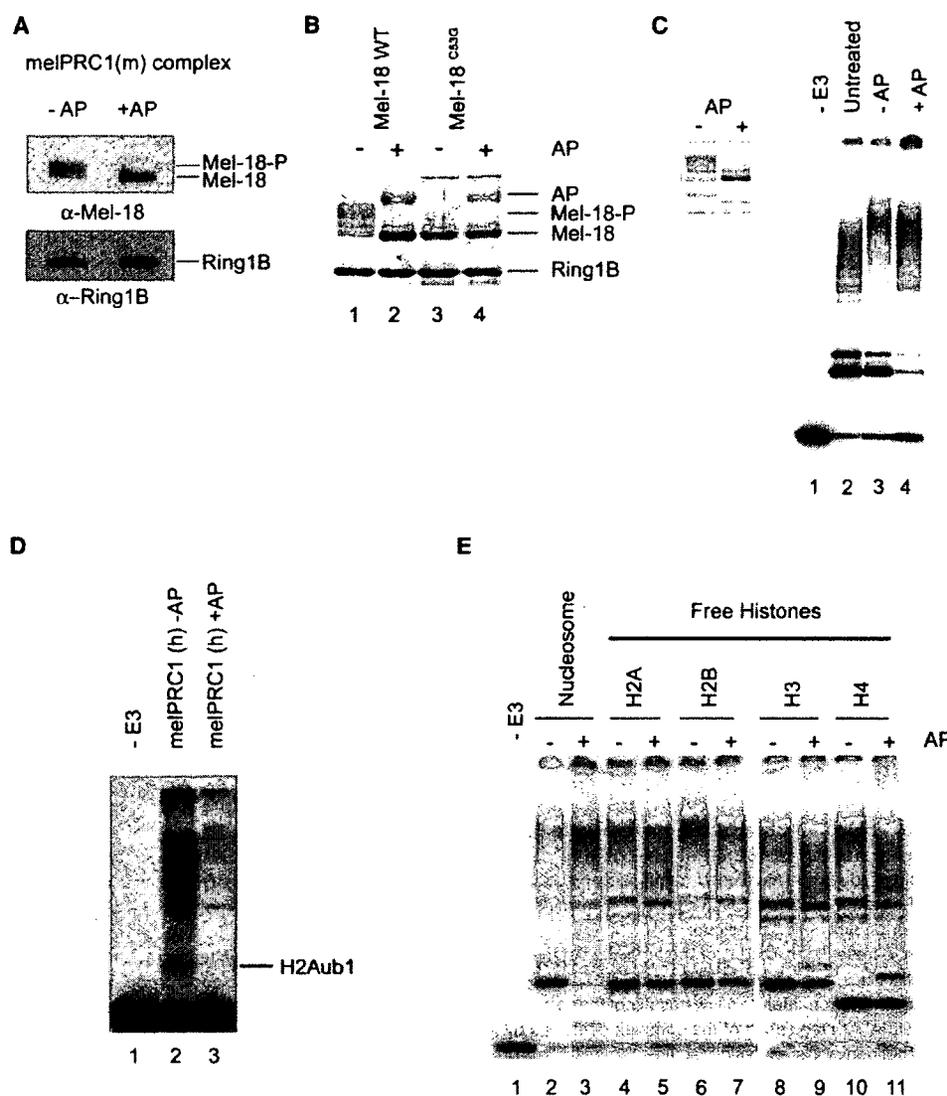
Figure 6. Phosphorylated Form of Mel-18 Directs Ring1B to Chromatin

(A) Mel-18 isolated from ES cells is phosphorylated. Western blot of Mel-18 complex melPRC1 isolated from BM3-3 cells (see Figure S1B). The complex was treated with AP or buffer for 1 hr and immunoblotted for Mel-18 or Ring1B antibody. Phosphorylated and nonphosphorylated forms of Mel-18 are indicated.

(B) Recombinant Ring1B/Mel-18, but not mutant Ring1B/Mel-18^{C53G}, complex is phosphorylated. Purified Ring1B/Mel-18 and Ring1B/Mel-18^{C53G} were treated with AP. AP, Ring1B, and the phosphorylated and nonphosphorylated forms of Mel-18 are indicated.

(C) Dephosphorylation of Mel18 ablates E3 ligase activity on nucleosomes. Left panel, Ring1B/Mel-18 complex treated, or not, with AP. Right panel, AP-treated and -untreated complex was assayed for ubiquitin ligase activity on nucleosome substrate.

(D) Dephosphorylation of the melPRC1 complex purified from 293T cells ablates E3 ligase activity on nucleosomes. AP-treated complex was assayed for ubiquitin ligase activity on nucleosome substrate.

(E) AP-treated Ring1B/Mel-18 retains the ability to ubiquitylate free histones. AP-treated and -untreated complex was assayed for ubiquitin ligase activity on nucleosomes or recombinant histones.

Functional Interchangeability of PRC1-like Complexes

The function of individual PRC1 components in higher organisms is poorly understood. Previous studies demonstrated that while Mel-18 and Bmi1 knockout mice have similar, though not identical, phenotypes (Akasaka et al., 1996, 1997; van der Lugt et al., 1994, 1996), the double knockout mouse embryos exhibit a more profound phenotype (Akasaka et al., 2001). This suggests that while these two proteins have independent functions, they may also exhibit some functional redundancy. This view is supported by our demonstration that Mel-18 can restore repression of Hox gene expression to Mel18$^{-/-}$Bmi1$^{-/-}$ ES cells.
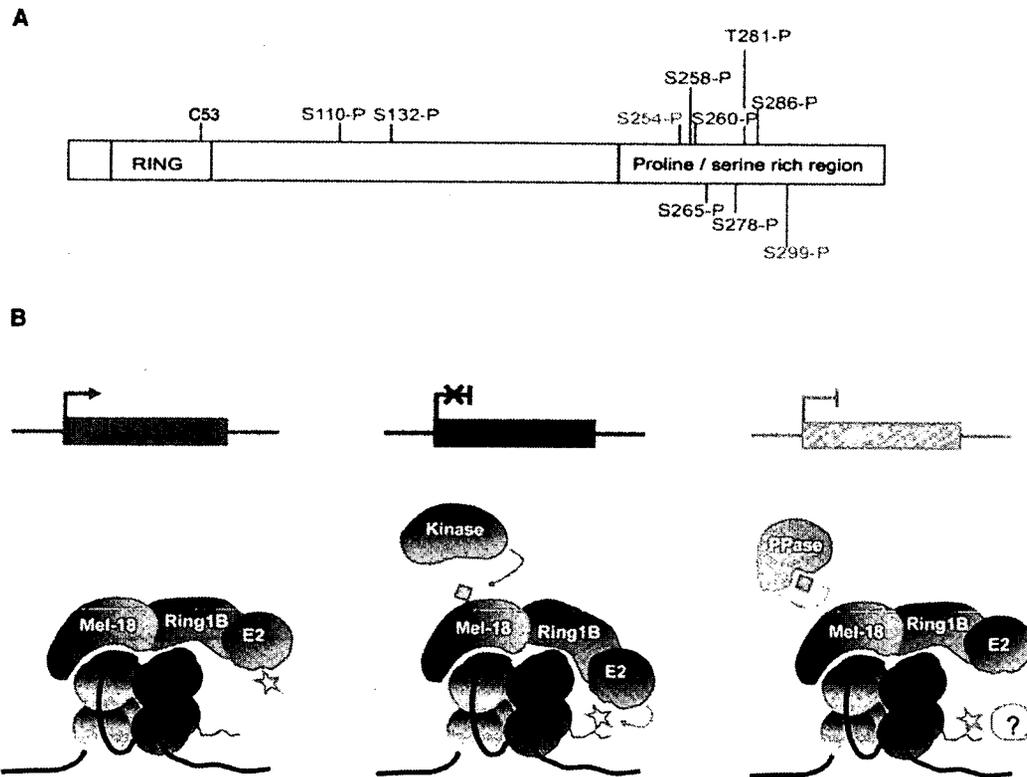
A

B

Figure 7. The Mel-18 Polycomb Complex Regulates Gene Expression

(A) Schematic representation of the Mel-18 protein showing the conserved RING domain containing the cysteine at position 53, and the proline/serine rich domain. Amino acid residues that have been identified by mass spectrometry analysis as being phosphorylated are shown. Red amino acids are phosphorylated in Mel-18 and conserved in Bmi1; green amino acids are phosphorylated in Mel-18 but are not conserved in Bmi1. Amino acid S132 was found to be a minor phosphorylated residue.

(B) Schematic diagram representing a model for the regulation of melPRC1 in H2A ubiquitylation. The unphosphorylated melPRC1 complex is proposed to bind chromatin. Phosphorylation of Mel-18 (blue diamond) by a putative Mel-18 kinase then brings about a conformational change, aligning the E2-conjugating enzyme appropriately to allow transfer of the ubiquityl group (orange star) to lysine 119 in the H2A tail. Mel-18 phosphorylation may represent the default state with regulation of the complex conferred by a phosphatase (PPase) that dephosphorylates Mel-18 and thereby derepresses associated target genes. Derepression requires removal of the ubiquityl group from H2A lysine 119 either by an active or passive mechanism (indicated with question mark).

In keeping with this notion, we find that MEL-18 (Mel-18) is part of a multiprotein complex with RING1/2 (Ring1A/B), HPH2a (mPh2), and CBX8 (mPc3), all of which also associate with BMI1 (Bmi1) (Levine et al., 2002; Wang et al., 2004) (Figure S1). However, since MEL-18 and BMI1 components are not found together in the same complex, they probably participate in distinct polycomb repressor complexes (melPRC1 and bmi1PRC1, respectively). This may explain the nonoverlapping functions of Mel-18 and Bmi1 defined in genetic experiments.

Mechanism of H2A Lysine 119 Ubiquitylation

Biochemical analyses of Ring1B/Bmi1 (Cao et al., 2005) and Ring1B/Mel-18 (this study) suggest that the two RING finger proteins synergize to form an active core that is sufficient for the efficient ubiquitylation of H2A lysine 119. The fact that Cao et al. (2005) failed to detect H2A ubiquitylation using Mel-18 in complex with Ring1B

may be attributable either to differences in the recombinant Mel-18 protein used in the two studies, for example the levels of phosphorylation at a specific site(s), or alternatively to differences in the assay conditions used.

In both subcomplexes, the Ring1B subunit is essential for ubiquitin transfer. It is generally held that RING finger E3 ligases provide a scaffold, which recruits both the ubiquitin-charged E2 enzyme and the substrate, juxtaposed so that transfer of ubiquitin can occur directly from E2 to substrate (Zheng et al., 2002). Our data suggest that Ring1B performs only the first of these functions, recruitment of the E2-conjugating enzyme. Consequently, mutations in Ring1B that alter the structure of the RING domain or interfere with the recruitment of the E2 abolish E3 function against chromatin or free histone substrates as well as autoubiquitylation. It is of note that we find no significant ubiquitin ligase activity with the Ring1B subunit alone.

On the other hand, a similar mutation (C53G) in the RING domain of Mel-18 abolishes ubiquitylation of nucleosome substrates, but not autoubiquitylation or the ubiquitylation of free histones. This suggests that while Mel-18 is not essential for E3 function per se, it is required to position the E3 ligase for the specific ubiquitylation of H2A lysine 119 in a chromatin context. Furthermore, the failure of the C53G mutant complex to ubiquitylate nucleosomes can be attributed to the fact that this mutant Mel-18 is not phosphorylated (see below). Extrapolating our observations, we suggest that other PSC paralogs, Bmi1, NSPc1, and MBLR, may carry out an equivalent function in targeting the E3 ligase activity of Ring1A/B to H2A lysine 119 in chromatin. The presence of the different PSC paralogs would allow the targeting of different genes by distinct PRC1-like complexes and/or a tight regulation via different cell signaling pathways.

Regulation of Polycomb Complexes by Phosphorylation

Recent studies have begun to identify how cell signaling pathways regulate gene repression by PcG proteins. Phosphorylation has been shown to reduce the HMTase activity of the PRC2 complex (Cha et al., 2005). Similarly, it has been suggested that phosphorylation of Bmi1 by MAPKAP kinase 3pK results in dissociation of bmiPRC1 from chromatin (Voncken et al., 2005). Jak-stat signaling has been shown to downregulate genes encoding PRC1 components, and this is important in transdifferentiation of imaginal disc cells in D. melanogaster (Lee et al., 2005). Our results provide a first example in which phosphorylation enhances activity of a polycomb complex, specifically stimulating recognition of the nucleosome substrate and ubiquitylation of H2A lysine 119 by the melPRC1 E3 ligase.

We identified nine phosphoserine and a single phosphothreonine residue in Mel-18. Sequence analysis reveals that these are consensus sites for multiple serine/ threonine kinases, including the casein kinase, cyclin-dependent kinase, and MAPK families. A previous study suggested that phosphorylation of Mel-18 can also be mediated by protein kinase C (Fujisaki et al., 2003). While we cannot rule this out, the majority of sites we identified are not a good consensus for this kinase family. The unambiguous identification of the regulatory kinase for melPRC1 awaits further study.

BMI1 can also be phosphorylated, but only at mitosis, correlating with its dissociation from chromatin (Voncken et al., 2005). Although this is functionally distinct from phosphorylation of Mel-18, it is possible that some of the sites of phosphorylation overlap. Two of the phosphoserine residues identified in Mel-18 (serines 254 and 299) are not conserved in Bmi1. Consequently, these sites may be good candidates for mediating unique functions of Mel-18.

Mel-18 is phosphorylated in Sf9 cells only when complexed with Ring1B (Figure 2C). It is of note that the C53G mutation in Mel-18, which abrogates phosphoryla-

tion, does not do so by disrupting this complex. As C53 is located in the RING domain of Mel-18, away from the majority of phosphorylation sites and at a residue that is highly conserved in Bmi1 paralogs, we speculate that C53G might alter the conformation of Mel-18 so that recognition by the regulatory kinase(s) is impaired.

How, then, does phosphorylation of Mel-18 impact on the H2A ubiquitylation activity of melPRC1? One possible mechanism is that phosphorylation of Mel-18 is required for the complex to bind to the surface of the nucleosome. Alternatively, phosphorylation may induce a conformational switch in Mel-18 already bound to a nucleosome, positioning Ring1B:E2 for transfer of ubiquitin onto H2A lysine 119. The fact that both phosphorylated and unphosphorylated Mel-18 is found in the chromatin fraction of HeLa cell nuclei perhaps favors the latter hypothesis (Figure S5 and Figure 7B). Structural analyses of phosphorylated and unphosphorylated forms of Mel-18/Bmi1 complexed with Ring1B should provide further insight.

In summary, our data suggest that evolution of the PSC homolog Mel-18 in higher organisms has allowed the acquisition of a distinct mode of regulating H2A ubiquitylation via phosphorylation. Although the biological function of Mel-18 phosphorylation remains to be determined, we envisage two possible models, which are illustrated in Figure 7B. First, a Mel-18 kinase may be regulated so as to repress target genes in response to a specific signal. Second, Mel-18 phosphorylation may be a default state, and regulation of a Mel-18 phosphatase could function to derepress target genes. In future work, identification of Mel-18 kinase/phosphatase activities should shed light on the biological function of Mel-18 phosphorylation in gene regulation by polycomb complexes.

EXPERIMENTAL PROCEDURES

Cell Lines and Derivations

BM3 cells were derived from Mel-18$^{-/+}$/Bmi1$^{-/+}$ heterozygote crosses using standard methods (H.K. and M.E., unpublished data). Generation of BM3 cell lines stably expressing Mel-18-FlagHis are described in the Supplemental Experimental Procedures. BM3 and BM3 transgenic cell lines were grown in DMEM (GIBCO) supplemented with 16% FCS (Autogen Bioclear, Calne, Wiltshire, UK), l-glutamine, nonessential amino acids, 50 IU/ml penicillin/streptomycin, 2-mercaptoethanol (GIBCO), and 1000 units/ml LIF (Chemicon) at 37°C and 5% CO_2.

HeLa cells were grown in DMEM supplemented with 10% FCS l-glutamine and 50 IU/ml penicillin/streptomycin at 37°C and 5% CO_2. Cell-cycle synchronization experiments were carried out as described in the Supplemental Experimental Procedures.

293T cells were cultured at 37°C in a humidified, 5% CO_2 atmosphere in DMEM supplemented to contain 10% FCS, 100 IU/ml penicillin, and 100 µg/ml streptomycin. 293T cells stably expressing human Mel-18-TAP, BMI-1-TAP, or TAP alone were generated as described in the Supplemental Experimental Procedures.

Purification of MEL-18 and BMI1 Complexes by TAP-Tag Purification

Human MEL-18 and BMI1 coding sequences were amplified from cDNA and cloned to produce an in-frame TAP tag, generating pGM-MEL-18cTAP or pQBT (BMI1-TAP). pGM-TAP expressing TAP alone was used as a negative control. 293T TAP, 293T, MEL-18TAP, and

293T-ER QBT cells were harvested and protein complexes purified as described in the Supplemental Experimental Procedures.

Purification of Recombinant Mel-18/Ring1B and Mutant Complexes

Full-length mouse Mel-18, Bmi1, and Ring1B were tagged with His_{12} and FLAG or HA and cloned into pDEST8 using the Gateway cloning system (Invitrogen). Mutant Mel-18-FlagHis and Ring1B-FlagHis were generated from the pDEST clones using site-directed mutagenesis kit (Stratagene). Recombinant baculovirus was generated using the Bac-to-Bac baculovirus system (Invitrogen). Wild-type virus vMel-18-HA, or vBmi1-HA, and vRing1B-FlagHis or the reciprocal tagged versions were coinfected in Sf9 insect cells for 60 hr. Complexes were purified as described in the Supplemental Experimental Procedures. Mutant Mel-18-FlagHis and wild-type Ring1B-HA or mutant Ring1B-FlagHis and wild-type Mel-18-HA were coinfected and grown as above. Mutant protein complexes were purified as wild-type complex.

Ubiquitylation Assays

Unless otherwise stated, reactions (25 µl) were performed as described in Mallery et al. (2002) using 300 ng E1 (Boston Biochem), 300 ng UbcH5c (affinity), 1 µg ubiquitin (Sigma), 1 µg purified E3, and 1.5 µg recombinant oligonucleosomes, or 2.5 µg of ES cell chromatin. ^{125}I-labeled products were visualized using the Molecular Dynamics Typhoon Phosphorimager and ImageQuaNT software. Where indicated, complexes were dephosphorylated by treatment with 2 U of AP (Roche 1 U/µl) in phosphatase buffer for 2 hr at 37°C.

Identification of Phosphorylation Sites

Approximately 1 µg of Mel-18 was separated by SDS-PAGE and stained with colloidal Coomassie. Mass spectrometry was carried out as described in the Supplemental Experimental Procedures.

Western Blot Analysis and Antibodies

Antibodies used in western blotting were Mel-18 (Abcam) 1:500, Ring1B (Atsuta et al., 2001) 1:500, Ring1A (Schoorlemmer et al., 1997) 1:500, mPh1 (Miyagishima et al., 2003) 1:10, cyclin A (Santa Cruz) 1:500, cyclin D (Santa Cruz) 1:200, cyclin E (Santa Cruz) 1:100, Lamin (Santa Cruz) 1:2000, and HDAC1 (Santa Cruz) 1:500. Westerns were carried out following protocols provided by the antibody supplier. Secondary antibodies were either sheep anti-mouse IgG HPR linked (GE Healthcare), donkey anti-rabbit Ig HPR linked (GE Healthcare), or donkey anti-goat IgG HRP linked (Santa Cruz). ECL detection (GE Healthcare) was carried out according to the manufacturer's recommendations.

Gene Expression Analysis

RNA from cells was isolated using TRIzol Reagent (Invitrogen) following the manufacturer's instructions. Removal of contaminating DNA using turbo DNase (Ambion) and cDNA synthesis using SuperScript III (Invitrogen) were carried out according to the manufacturer's guidelines. Quantitative real-time PCR was carried out using SYBR Green (Bio-Rad) following the manufacturer's instructions. Data were normalized to the average obtained for two house keeping genes GAPDH and HMBS. Genes analyzed were Hoxa1, Hoxa5, Hoxd4, Hoxd8, and the control gene Oct-4. Primer sequences are provided in Table S2. Gene expression levels for the three transgenic cells lines BM3-1, BM3-2, and BM3-3 are represented as a ratio of the parental cell line BM3.

Chromatin Immunoprecipitation

ChIP experiments were carried out as described below. Cells (1×10^8) were fixed with 1% formaldehyde for 10 min at room temperature. The reaction was stopped with a final concentration of 125 mM Glycine. Whole-cell extracts were then sonicated to produce an average DNA fragment size of around 500 bp. Chromatin (150 µg) was used in

each immunoprecipitation reaction carried out with either anti-Mel-18 (Santa Cruz), anti-Ring1B (Atsuta et al., 2001), or the appropriate control IgG antibodies overnight at 4°C with rotation. Beads were washed four times with wash buffer 1 and once with final wash buffer. Immunoprecipitated chromatin was eluted from the beads in elution buffer and reverse crosslinked overnight. The precipitated DNA was dissolved in 100 µl of TE. ChIP DNA was analyzed by real-time PCR using SYBR green (Bio-Rad) following the manufacturer's instructions. Enrichment was normalized to input DNA. Primers utilized are shown in Table S3.

Supplemental Data

Supplemental Data include Supplemental Experimental Procedures, seven figures, three tables, and Supplemental References and can be found with this article online at http://www.molecule.org/cgi/content/full/28/1/107/DC1/.

REFERENCES

Akasaka, T., Kanno, M., Balling, R., Mieza, M.A., Taniguchi, M., and Koseki, H. (1996). A role for mel-18, a Polycomb group-related vertebrate gene, during theanteroposterior specification of the axial skeleton. Development 122, 1513–1522.

Akasaka, T., Tsuji, K., Kawahira, H., Kanno, M., Harigaya, K., Hu, L., Ebihara, Y., Nakahata, T., Tetsu, O., Taniguchi, M., and Koseki, H. (1997). The role of mel-18, a mammalian Polycomb group gene, during IL-7-dependent proliferation of lymphocyte precursors. Immunity 7, 135–146.

Akasaka, T., van Lohuizen, M., van der Lugt, N., Mizutani-Koseki, Y., Kanno, M., Taniguchi, M., Vidal, M., Alkema, M., Berns, A., and Koseki, H. (2001). Mice doubly deficient for the Polycomb group genes Mel18 and Bmi1 reveal synergy and requirement for maintenance but not initiation of Hox gene expression. Development 128, 1587–1597.

Akasaka, T., Takahashi, N., Suzuki, M., Koseki, H., Bodmer, R., and Koga, H. (2002). MBLR, a new RING finger protein resembling mammalian Polycomb gene products, is regulated by cell cycle-dependent phosphorylation. Genes Cells 7, 835–850.

Atsuta, T., Fujimura, S., Moriya, H., Vidal, M., Akasaka, T., and Koseki, H. (2001). Production of monoclonal antibodies against mammalian Ring1B proteins. Hybridoma 20, 43–46.

Ben-Saadon, R., Zaaroor, D., Ziv, T., and Ciechanover, A. (2006). The polycomb protein Ring1B generates self atypical mixed ubiquitin chains required for its in vitro histone H2A ligase activity. Mol. Cell 24, 701–711.

Brunk, B.P., Martin, E.C., and Adler, P.N. (1991). Drosophila genes Posterior Sex Combs and Suppressor two of zeste encode proteins with homology to the murine bmi-1 oncogene. Nature 353, 351–353.

Brzovic, P.S., Keeffe, J.R., Nishikawa, H., Miyamoto, K., Fox, D., 3rd, Fukuda, M., Ohta, T., and Klevit, R. (2003). Binding and recognition in

the assembly of an active BRCA1/BARD1 ubiquitin-ligase complex. Proc. Natl. Acad. Sci. USA 100, 5646–5651.

Buchwald, G., van der Stoop, P., Weichenrieder, O., Perrakis, A., van Lohuizen, M., and Sixma, T.K. (2006). Structure and E3-ligase activity of the Ring-Ring complex of polycomb proteins Bmi1 and Ring1b. EMBO J. 25, 2465–2474.

Cao, R., Wang, L., Wang, H., Xia, L., Erdjument-Bromage, H., Tempst, P., Jones, R.S., and Zhang, Y. (2002). Role of histone H3 lysine 27 methylation in Polycomb-group silencing. Science 298, 1039–1043.

Cao, R., Tsukada, Y., and Zhang, Y. (2005). Role of Bmi-1 and Ring1A in H2A ubiquitylation and Hox gene silencing. Mol. Cell 20, 845–854.

Cha, T.L., Zhou, B.P., Xia, W., Wu, Y., Yang, C.C., Chen, C.T., Ping, B., Otte, A.P., and Hung, M.C. (2005). Akt-mediated phosphorylation of EZH2 suppresses methylation of lysine 27 in histone H3. Science 310, 306–310.

Chen, A., Kleiman, F.E., Manley, J.L., Ouchi, T., and Pan, Z.Q. (2002). Autoubiquitination of the BRCA1*BARD1 RING ubiquitin ligase. J. Biol. Chem. 277, 22085–22092.

Czermin, B., Melfi, R., McCabe, D., Seitz, V., Imhof, A., and Pirrotta, V. (2002). Drosophila enhancer of Zeste/ESC complexes have a histone H3 methyltransferase activity that marks chromosomal Polycomb sites. Cell 111, 185–196.

de Napoles, M., Mermoud, J.E., Wakao, R., Tang, Y.A., Endoh, M., Appanah, R., Nesterova, T.B., Silva, J., Otte, A.P., Vidal, M., et al. (2004). Polycomb group proteins Ring1A/B link ubiquitylation of histone H2A to heritable gene silencing and X inactivation. Dev. Cell 7, 663–676.

Francis, N.J., Saurin, A.J., Shao, Z., and Kingston, R.E. (2001). Reconstitution of a functional core polycomb repressive complex. Mol. Cell 8, 545–556.

Fritsch, C., Beuchle, D., and Muller, J. (2003). Molecular and genetic analysis of the Polycomb group gene Sex combs extra/Ring in Drosophila. Mech. Dev. 120, 949–954.

Fujimura, Y., Isono, K., Vidal, M., Endoh, M., Kajita, H., Mizutani-Koseki, Y., Takihara, Y., van Lohuizen, M., Otte, A., Jenuwein, T., et al. (2006). Distinct roles of Polycomb group gene products in transcriptionally repressed and active domains of Hoxb8. Development 133, 2371–2381.

Fujisaki, S., Ninomiya, Y., Ishihara, H., Miyazaki, M., Kanno, R., Asahara, T., and Kanno, M. (2003). Dimerization of the Polycomb-group protein Mel-18 is regulated by PKC phosphorylation. Biochem. Biophys. Res. Commun. 300, 135–140.

Gearhart, M.D., Corcoran, C.M., Wamstad, J.A., and Bardwell, V.J. (2006). Polycomb group and SCF ubiquitin ligases are found in a novel BCOR complex that is recruited to BCL6 targets. Mol. Cell. Biol. 26, 6880–6889.

Hashizume, R., Fukuda, M., Maeda, I., Nishikawa, H., Oyake, D., Yabuki, Y., Ogata, H., and Ohta, T. (2001). The RING heterodimer BRCA1-BARD1 is a ubiquitin ligase inactivated by a breast cancer-derived mutation. J. Biol. Chem. 276, 14537–14540.

Jorgensen, H.F., Giadrossi, S., Casanova, M., Endoh, M., Koseki, H., Brockdorff, N., and Fisher, A.G. (2006). Stem cells primed for action: polycomb repressive complexes restrain the expression of lineage-specific regulators in embryonic stem cells. Cell Cycle 13, 1411–1414.

Klymenko, T., Papp, B., Fischle, W., Kocher, T., Schelder, M., Fritsch, C., Wild, B., Wilm, M., and Muller, J. (2006). A Polycomb group protein complex with sequence-specific DNA-binding and selective methyl-lysine-binding activities. Genes Dev. 20, 1110–1122.

Kuzmichev, A., Nishioka, K., Erdjument-Bromage, H., Tempst, P., and Reinberg, D. (2002). Histone methyltransferase activity associated with a human multiprotein complex containing the Enhancer of Zeste protein. Genes Dev. 16, 2893–2905.

Kuzmichev, A., Jenuwein, T., Tempst, P., and Reinberg, D. (2004). Different EZH2-containing complexes target methylation of histone H1 or nucleosomal histone H3. Mol. Cell 14, 183–193.

Lee, N., Maurange, C., Ringrose, L., and Paro, R. (2005). Suppression of Polycomb group proteins by JNK signalling induces transdetermination in Drosophila imaginal discs. Nature 438, 234–237.

Levine, S.S., Weiss, A., Erdjument-Bromage, H., Shao, Z., Tempst, P., and Kingston, R.E. (2002). The core of the polycomb repressive complex is compositionally and functionally conserved in flies and humans. Mol. Cell. Biol. 22, 6070–6078.

Li, Z., Cao, R., Wang, M., Myers, M.P., Zhang, Y., and Xu, R.M. (2006). Structure of a Bmi-1-Ring1B polycomb group ubiquitin ligase complex. J. Biol. Chem. 281, 20643–20649.

Mallery, D.L., Vandenberg, C.J., and Hiom, K. (2002). Activation of the E3 ligase function of the BRCA1/BARD1 complex by polyubiquitin chains. EMBO J. 21, 6755–6762.

Miyagishima, H., Isono, K., Fujimura, Y., Iyo, M., Takihara, Y., Masumoto, H., Vidal, M., and Koseki, H. (2003). Dissociation of mammalian Polycomb-group proteins, Ring1B and Rae28/Ph1, from the chromatin correlates with configuration changes of the chromatin in mitotic and meiotic prophase. Histochem. Cell Biol. 120, 111–119.

Muller, J., Hart, C.M., Francis, N.J., Vargas, M.L., Sengupta, A., Wild, B., Miller, E.L., O'Connor, M.B., Kingston, R.E., and Simon, J.A. (2002). Histone methyltransferase activity of a Drosophila Polycomb group repressor complex. Cell 111, 197–208.

Ogawa, H., Ishiguro, K., Gaubatz, S., Livingston, D.M., and Nakatani, Y. (2002). A complex with chromatin modifiers that occupies E2F- and Myc-responsive genes in G0 cells. Science 296, 1132–1136.

Saurin, A.J., Shao, Z., Erdjument-Bromage, H., Tempst, P., and Kingston, R.E. (2001). A Drosophila Polycomb group complex includes Zeste and dTAFII proteins. Nature 412, 655–660.

Schoorlemmer, J., Marcos-Gutierrez, C., Were, F., Martinez, R., Garcia, E., Satijn, D.P., Otte, A.P., and Vidal, M. (1997). Ring1A is a transcriptional repressor that interacts with the Polycomb-M33 protein and is expressed at rhombomere boundaries in the mouse hindbrain. EMBO J. 16, 5930–5942.

Schwartz, Y.B., and Pirrotta, V. (2007). Polycomb silencing mechanisms and the management of genomic programmes. Nat. Rev. Genet. 8, 9–22.

Shao, Z., Raible, F., Mollaaghababa, R., Guyon, J.R., Wu, C.T., Bender, W., and Kingston, R.E. (1999). Stabilization of chromatin structure by PRC1, a Polycomb complex. Cell 98, 37–46.

Tonkin, E., Hagan, D.M., Li, W., and Strachan, T. (2002). Identification and characterisation of novel mammalian homologues of Drosophila polyhomeotic permits new insights into relationships between members of the polyhomeotic family. Hum. Genet. 111, 435–442.

van der Lugt, N.M., Domen, J., Linders, K., van Roon, M., Robanus-Maandag, E., te Riele, H., van der Valk, M., Deschamps, J., Sofroniew, M., van Lohuizen, M., et al. (1994). Posterior transformation, neurological abnormalities, and severe hematopoietic defects in mice with a targeted deletion of the bmi-1 proto-oncogene. Genes Dev. 8, 757–769.

van der Lugt, N.M., Alkema, M., Berns, A., and Deschamps, J. (1996). The Polycomb-group homolog Bmi-1 is a regulator of murine Hox gene expression. Mech. Dev. 58, 153–164.

van Lohuizen, M., Frasch, M., Wientjens, E., and Berns, A. (1991). Sequence similarity between the mammalian bmi-1 proto-oncogene and the Drosophila regulatory genes Psc and Su(z)2. Nature 353, 353–355.

Voncken, J.W., Niessen, H., Neufeld, B., Rennefahrt, U., Dahlmans, V., Kubben, N., Holzer, B., Ludwig, S., and Rapp, U.R. (2005). MAPKAP kinase 3pK phosphorylates and regulates chromatin association of the polycomb group protein Bmi1. J. Biol. Chem. 280, 5178–5187.

211

Wang, H., Wang, L., Erdjument-Bromage, H., Vidal, M., Tempst, P., Jones, R.S., and Zhang, Y. (2004). Role of histone H2A ubiquitination in Polycomb silencing. Nature 431, 873–878.

Wei, J., Zhai, L., Xu, J., and Wang, H. (2006). Role of Bmi1 in H2A ubiquitylation and Hox gene silencing. J. Biol. Chem. 281, 22537–22544.

West, M., and Bonner, W. (1980). Histone 2A, a heteromorphous family of eight protein species. Biochemistry 19, 3238–3245.

Yamaki, M., Isono, K., Takada, Y., Abe, K., Akasaka, T., Tanzawa, H., and Koseki, H. (2002). The mouse Edr2 (Mph2) gene has two forms of mRNA encoding 90- and 36-kDa polypeptides. Gene 288, 103–110.

Zheng, N., Schulman, B.A., Song, L., Miller, J.J., Jeffrey, P.D., Wang, P., Chu, C., Koepp, D.M., Elledge, S.J., Pagano, M., et al. (2002). Structure of the Cul1-Rbx1-Skp1-F boxSkp2 SCF ubiquitin ligase complex. Nature 416, 703–709.

Polycomb complexes regulate cellular senescence by repression of *ARF* in cooperation with E2F3

Jun Miki[1], Yu-ichi Fujimura[2], Haruhiko Koseki[2] and Takehiko Kamijo[1,3,*]

[1]*Department of Pediatrics, Shinshu University School of Medicine, Matsumoto, Nagano 390-8621, Japan*
[2]*Developmental Genetics Group, RIKEN Research Center for Allergy and Immunology, Tsurumi-ku, Yokohama 230-0045, Japan*
[3]*Division of Biochemistry, Chiba Cancer Center Research Institute, 666-2 Nitona, Chuoh-ku, Chiba 260-8717, Japan*

Cellular senescence is a program in normal cells triggered in response to various types of stress that cells experience when they are explanted into culture. In this study, functional analyses on the role of the class II polycomb complex in cellular senescence were performed using mouse embryo fibroblasts (MEFs) with a genetically deleted member of the complex, *Mel18*. *Mel18*-null MEFs undergo typical premature senescence accompanied by the up-regulation of ARF/p53/ p16^{INK4a} and decrease of Ring1b/Bmi1. Our results demonstrated that *ARF* or *p53* deletion cancels the senescence in *Mel18*-null MEFs, and the fact that p16^{INK4a} is up-regulated in double-null MEFs suggests that the ARF/p53 pathway plays a central role in stress-induced senescence. The *in vivo* binding of Ring1b and E2F3b to the *ARF* promoter decreased progressively in senescence, and *Mel18* inactivation accelerated the exfoliation of Ring1b/E2F3b from the promoter sequence, indicating the cooperation of polycombs/E2F3b on ARF expression and cellular senescence. Taken together, it seems that class II polycomb proteins and E2F3b dually control cellular senescence via the ARF/p53 pathway.

Introduction

Cellular senescence is a fundamental cellular program that is activated in various stress situations and acts to prevent further cell proliferation. As a population of cells is propagated in culture, cells are exposed to various extrinsic and intrinsic stresses, and the cell population gradually stops dividing. In contrast to 'replicative senescence' which stands for the widely accepted model of a terminal growth arrest due to telomere attrition, it is now clear that many stimuli, including oxidative stress, DNA damage and oncogene activation cause an acutely inducible, 'premature' form of cellular senescence which is independent of telomere attrition. Cellular senescence is considered to play an important role in tumor suppression and to contribute to organismal aging. In fact, two definitive tumor suppressor pathways, ARF/MDM2/ p53 and p16^{INK4a}/Rb, have been shown to play critical roles in the induction of cellular senescence (Sherr & DePinho 2000).

Polycomb group (PcG) genes were first identified in *Drosophila* as a group of genes required to maintain the stable repression of Hox cluster genes during development. An increasing number of mammalian genes structurally and functionally related to *Drosophila* PcG genes have been identified, including *Mel18*, *Bmi1*, *M33* and *rae28*, and shown to form multimeric protein complexes associated with chromatin (Levine *et al.* 2004). There are increasing lines of evidence that PcG proteins themselves affect cellular proliferation and cellular senescence. Targeted disruption of *Bmi1*, *Mel18*, *rae28* and *M33*, members of the class II PcG complex, leads to proliferation defects in hematopoietic stem cells (Lessard *et al.* 1999; Ohta *et al.* 2002; Park *et al.* 2003; Iwama *et al.* 2004) and mouse embryo fibroblasts (MEF) (Bmi1, Jacobs *et al.* 1999; M33, Core *et al.* 1997; Phc2, Isono *et al.* 2005), indicating that inactivation of these PcGs results in cell proliferation failure. Premature senescence of MEFs derived from *Bmi1-*, *M33-* and *Phc2-*null mice has been shown to be mediated by de-repression of the central mediators of senescence signals, p19^{ARF} and p16^{INK4a}, which are encoded by the *p15^{INK4b}/p19^{ARF}/p16^{INK4a}* genomic region (*INK4/ARF region*). The molecular mechanism underlying the transcriptional regulation of these genes by mammalian PcG

complexes, however, has not yet been appropriately addressed, except for physical interactions of Bmi1 and Phc2 gene products with $p19^{ARF}$ and $p16^{INK4a}$ genomic regions (Jacobs *et al.* 1999; Itahana *et al.* 2003; Isono *et al.* 2005). The Mel18 component of PcG complexes shares homologous amino acid sequences with Bmi1 proteins and interacts with almost the same set of mammalian PcG proteins (Jacobs & van Lohuizen 2002). Accordingly, *Mel18*- and *Bmi1*-knockout mice exhibited similar phenotypes in axial and hematopoietic systems, and phenotypic analyses of *Mel18/Bmi1* double-knockout mice revealed their functional redundancy. However, it is also true that the molecular functions of Mel18 and Bmi1 are not totally identical since their deficient phenotypes were found to be mutually distinct in various aspects (van der Lugt *et al.* 1994; Akasaka *et al.* 1996). This was supported by recent biochemical analysis that Bmi1 enhances Ring1b-mediated ubiquitinylation of histone H2A more efficiently than Mel18 (Cao *et al.* 2005). Although it has been reported that *Mel18*-null MEFs undergo premature senescence similar to *Bmi1* mutants, the molecular mechanisms underlying Mel18-mediated regulation of senescence remain to be elucidated (Kanno *et al.* 1995; Jacobs *et al.* 1999), particularly, whether its action involves the transcriptional regulation of $p19^{ARF}$ and $p16^{INK4a}$, as in Bmi1.

E2F proteins have been shown to control the expression of a large number of genes involved in DNA replication, cell cycle progression and cell fate determination (Sears & Nevins 2002). The E2F family is composed of six distinct gene products (E2F1–E2F6) that form heterodimeric complexes with partners of the DP family, DP-1 and DP-2. E2F1–E2F3 act as positive regulators of transcription, whereas E2F4–E2F6 function primarily as transcriptional repressors. E2F3 protein appears to be particularly important for cell proliferation, as seen from the inhibition of E2F3 activity by antibody microinjection (Leone *et al.* 1998). Furthermore, the loss of E2F3a+b is shown to de-repress ARF, triggering the activation of p53 and expression of $p21^{Cip1/Waf1}$ (Humbert *et al.* 1998). *ARF* mutation in E2F3a+b mutants suppresses $p21^{Cip1/Waf1}$, and rescues the known cell cycle re-entry defect of mutant MEFs. Moreover, in wild-type MEFs, the *ARF* promoter is predominantly occupied by E2F3b, which differs from E2F3a in its N-terminal sequence, suggesting that transcription of *ARF* is negatively controlled primarily by E2F3b in cell culture (Aslanian *et al.* 2004). In that study, the authors suggested the presence of E2F3 co-repressors cooperating in the regulation of *ARF* transcription. A recent study by Core *et al.* (2004) has shown that the premature senescence of *M33*-null MEFs is canceled by a transdominant negative form of E2F (E2F-DB). This observation suggests that E2F family proteins mediate de-repression of ARF/$p16^{INK4a}$ expression in MEFs deficient in genes encoding components of class II PcG complexes; however, the molecular mechanisms underlying the functional correlation between PcG complexes and E2F3s are not fully known.

In the present study, we first addressed the role of Mel18 in the cellular senescence of MEFs. Severe proliferation disturbance, up-regulation of $p19^{ARF}$/p53/$p16^{INK4a}$ and decrease of Ring1b/Bmi1 were observed in *Mel18*-null MEFs. Genetic deletion of *ARF* or *p53* cancelled premature senescence, confirming the importance of the ARF/p53 pathway in senescence. We further analyzed the physical associations of PcG and E2F3 proteins with the INK4/ARF region in wild-type and *Mel18*-null MEFs by chromatin immunoprecipitation (ChIP) assays. Associations of Ring1b components with class II PcG complexes and E2F3b with the *ARF* promoter region were found to be collinearly impaired in *Mel18*-null MEFs. It is thus presumed that the lack of a single PcG component may affect the amount of class II PcG complex and the binding of class II complexes with the *ARF* promoter region, which may in turn affect the association of E2F3b and result in de-repression of the *ARF* gene. Taken together, the association of E2F3b with the *ARF* promoter, which is regulated at least in part by PcG complexes, may be one of the essential parameters that mediate cellular proliferation and senescence in MEFs.

Results

Mel18 inactivation impairs cell growth of MEFs

Normally, the growth of passaged wild-type MEFs gradually decreases in sequential *in vitro* culture (Kamijo *et al.* 1997), but *Mel18*-null MEFs grew very slowly from the beginning of culture and soon stopped dividing, as reported previously (Fig. 1a; Jacobs *et al.* 1999). Consistent with this, the proliferation of *Mel18*-null MEFs was significantly slower than their wild-type littermate-derived MEFs in growth speed assays at passage-3 (Fig. 1b). Indicative of premature senescence, we found that *Mel18*-null MEFs exhibited strong positive staining for the SA-β-Gal enzyme as well as *Bmi1*-null MEFs, whereas only a few cells stained positive for the SA-β-Gal enzyme in wild-type MEF controls (Fig. 1c). In addition, *Mel18*-null and *Bmi1*-null MEFs exhibited enlarged nuclei and cell bodies.

To examine whether the proliferation failure of *Mel18*-null cells was not caused by the acceleration of apoptotic cell death, we treated *Mel18*-null and wild-type MEFs with serum starvation, ionizing irradiation and DNA topoisomerase II inhibitor, VP-16 and then assessed apoptotic cell death by FACS. There was no significant
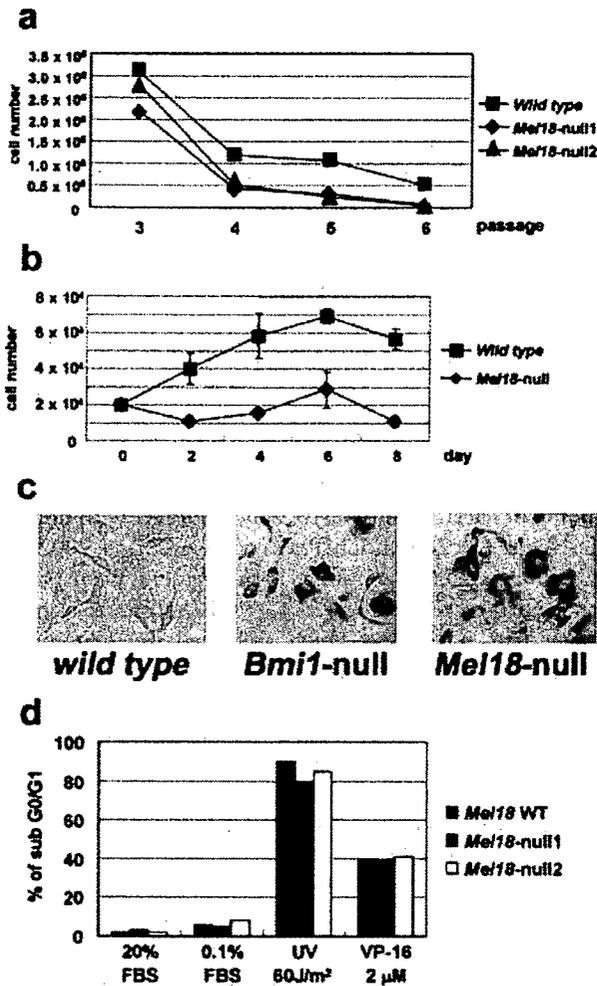
Figure 1 *Mel18*-null MEFs showed proliferation failure accompanied by ARF/p53/p16^{INK4a} activation. (a) Each data point represents the average of a minimum of three separate culture experiments as indicated in Experimental procedures. (b) Growth speeds were determined by growth speed assays for cells taken at passage-3.The values represent average and standard deviations of triplicate cultures. (c) Passage-5 MEFs, which had been cultured by the protocol used in Fig. 1a, were counted and seeded on a 3-cm diameter culture dish. Senescence-associated β-galactosidase enzyme activity was studied as indicated in Experimental procedures. (d) Cells were treated with indicated stresses (low serum, UV and VP-16) for 24 h and then % of sub-G0/G1 was determined by FACScan.

difference in the rate of apoptosis against these stresses between *Mel18*-null cells and controls (Fig. 1d); therefore, mitotic failure of *Mel18*-null MEFs was shown to not involve the acceleration of apoptotic outbursts.

## Effects of Mel18 inactivation on INK4/ARF/p53 pathways and class II polycomb proteins

We then performed Western blot analysis of the molecules negatively controlling cell cycle progression. In wild-type MEFs, proliferative capacity was found to dwindle and eventually cease, and the cells expressed elevated levels of negative cell cycle regulators, including the CDK inhibitors p16^{INK4a} and p21$^{Cip1/Waf1}$, the p53 inducer p19^{ARF} and p53 itself (Kamijo *et al.* 1997; Zindy *et al.* 1998). In the passaged cells, p19^{ARF}, p53, p16^{INK4a} and p53-downstream p21$^{Cip1/Waf1}$/MDM2 were already up-regulated in *Mel18*-null MEFs compared with their wild-type littermate-derived MEFs (Fig. 2a).We studied the expression of *ARF* mRNA and *p16^{INK4a}* mRNA by RT-PCR assay (Fig. 2b). Up-regulation of *ARF* and *p16^{INK4a}* mRNA expression was clearly observed in *Mel18*-null MEFs compared with wild-type littermate MEFs, indicating that the transcription of cell cycle-negative regulators was increased in *Mel18*-null MEFs.

Next, we analyzed the effect of Mel18 knockout on class II PcG proteins and E2F3 proteins. Class II PcG proteins, Ring1b and Bmi1 were clearly down-regulated in *Mel18*-null MEFs although E2F3a and E2F3b were hardly modulated (Fig. 2c).The down-regulation of PcG proteins seemed to be caused at the protein level since mRNA expression of Ring1b and Bmi1 was similar in both wild-type and *Mel18*-null MEFs (Fig. 2d).

Loss of ARF or p53 reverses proliferation failure of *Mel18*-null MEFs

We generated and analyzed *Mel18/ARF-* and *Mel18/p53*-knockout mice as described in Experimental procedures to address the effects of ARF or p53 on premature senescence in *Mel18*-null MEFs. Deletion of *ARF* or *p53* with the *Mel18*-null background rescued premature growth arrest in modified 3T9 assays (Fig. 3a) and growth speed retardation of passage-6 MEFs (Fig. 3c) due to *Mel18* loss. Since the proliferation of *ARF/Mel18* and *p53/Mel18* double-null MEFs was arrested by re-induction of ARF and p53 by retroviruses, respectively, as observed to a similar extent in *ARF* and *p53* single-null MEFs, activation of ARF and p53 may be a rate-limiting process to mediate growth arrest in *Mel18*-null MEFs (Fig. 3c-1 and c-2). Intriguingly, the proliferation of *ARF-* or *p53*-single-null MEFs was faster than those of ARF/Mel18- or p53/Mel18-double-null MEFs, respectively (Fig. 3c-1 and c-2, mock transfection).

Western blot analysis of passage-12 MEFs in modified 3T9 experiments indicated a significant reduction of p53-downstream molecules, p21$^{Cip1/Waf1}$ and MDM2, in
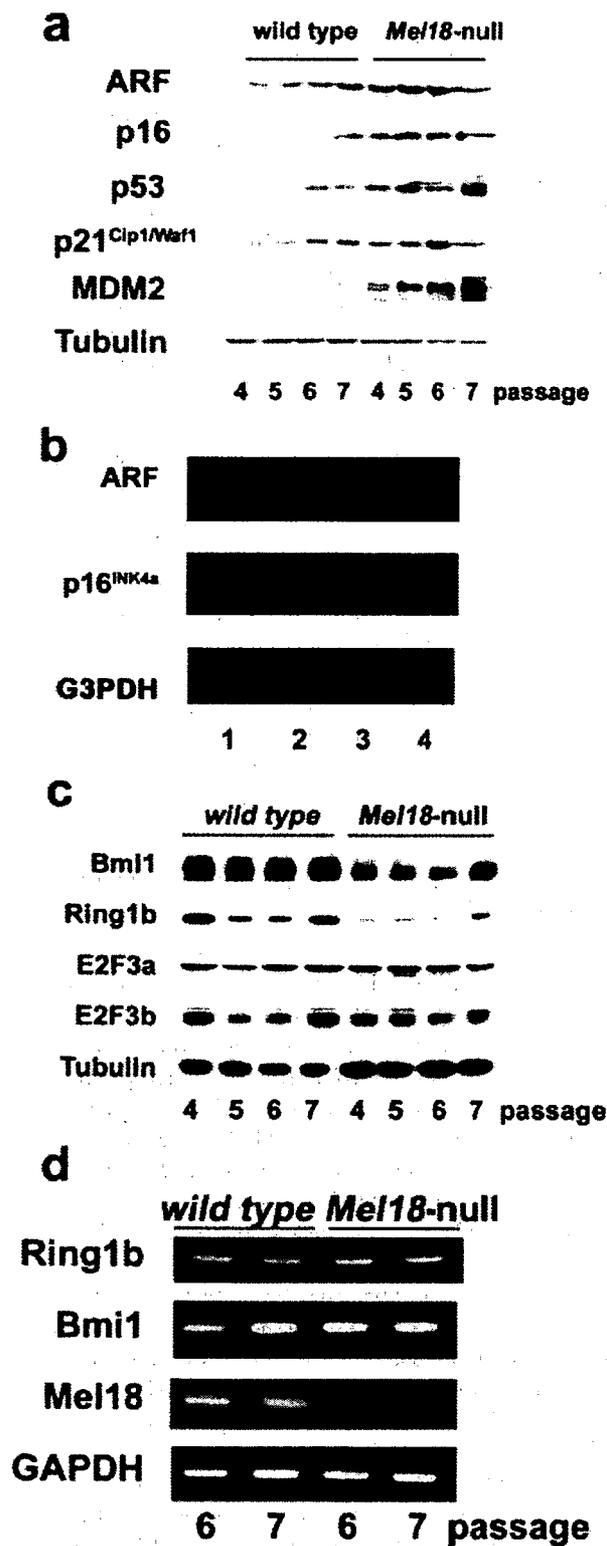
both double-null MEFs. In contrast, the expression of $p16^{INK4a}$ was even increased in double-null cells compared to Mel18 single mutants (Fig. 3b; Kamijo et al. 1997; Zindy et al. 1998). These findings suggest that ARF and p53 are key players in the premature senescence of Mel18-null cells, and $p21^{Cip1/Waf1}$ may be an especially important effector in arrested Mel18-null cells.

Binding of PcG proteins to $p15^{INK4b}/p19^{ARF}/p16^{INK4a}$ genomic locus

Recently, we reported the binding of Phc2, which interacts with Mel18, to $p16^{INK4a}$ exons 1 and 2 genomic sequences in developing embryos (Isono et al. 2005); however, it has not been addressed whether this association involves PcG complexes. We thus examined the binding of Mel18 and Ring1b, which interact with both Mel18 and Phc2, with ChIP assays (Suzuki et al. 2002). Immunoprecipitated genomic DNA fragments from 11.5 dpc embryos were subjected to PCR reactions using primer pairs (Table 2), which amplified the genomic regions schematically indicated in Fig. 4a. The region including the E2F site in the ARF promoter region was characterized by strong binding with Ring1b, although there was weak binding with Mel18 (Fig. 4b). In contrast, the p16 promoter sequence was characterized by abundantly bound Ring1b and Mel18 (Fig. 4c). Species-matched immunoglobulins were negative controls for ChIP experiments (Fig. 4b–d). In summary, although Ring1b association was seen in all regions examined, Mel18 binding was missing from several regions (Fig. 4a). This may localize the physical association of PcG complexes to an approximately 20 kb genomic region in and around the $p15^{INK4b}/p19^{ARF}/p16^{INK4a}$ locus, and suggest a model of compositional heterogeneity of PcG complexes.

Figure 2 Mel18 deficiency induces ARF/p16INK4a transcription and reduces class II PcG protein amounts. (a and c) MEFs grown by the indicated culture protocol used in Fig. 1a were sampled at each passage for the indicated protein expression by SDS PAGE/direct Western blotting. (b) RT-PCR amplification of $p16^{INK4a}$ and $p19^{ARF}$ RNAs. Lane 1 shows the products recovered from equal amounts of p53-mutated MEFs-derived RNA used as a positive control. Lane 2 shows the results with no templates. Lanes 3 and 4 show results of wild-type MEFs and Mel18-null MEFs, respectively, at passage-6. ARF, $p16^{INK4a}$ and G3PDH were amplified as described in Experimental procedures. (d) RT-PCR amplification of PcGs. Total RNAs were extracted from wild-type or Mel18-null MEFs and then the expressions of Bmi1, Ring1b and Mel18 were studied by RT-PCR.
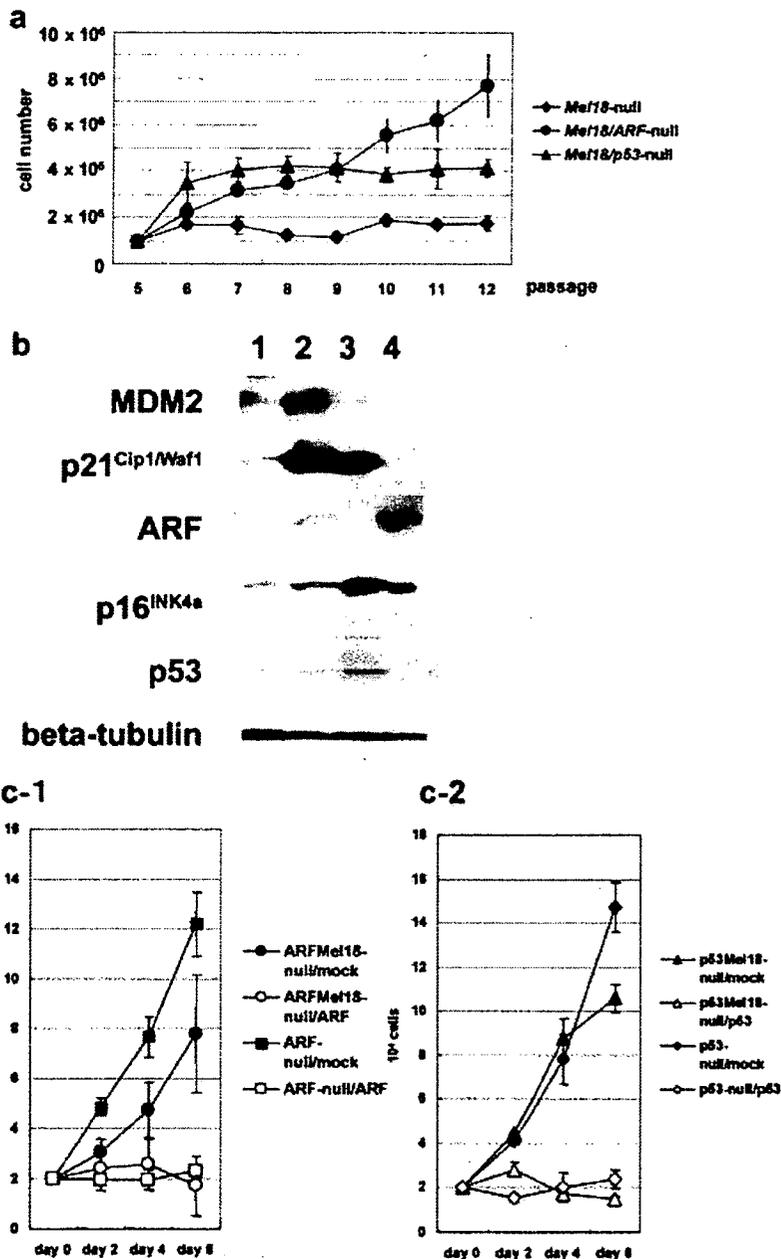
Figure 3 ARF or p53 inactivation cancels cellular senescence in *Mel18*-null MEFs. (a) Cells were passaged at 3-day intervals, counted, and re-plated according to the modified 3T9 protocol. Each data point represents the average of a minimum of three separate assays. Genotypes: *Mel18*-null (filled diamond), *ARF/Mel18*-null (filled circle) and *p53/Mel18*-null (filled triangle). (b) MEFs cultured by the modified 3T9 protocol were sampled at passage-12 for the indicated protein expression by direct Western blotting. Equal quantities of total cell lysate (30 µg of protein) were loaded per lane of mini-SDS-PAGE gel, transferred onto PVDF membranes, and probed with the anti-bodies indicated in the left margin. Lane 1, wild-type; lane 2, *Mel18*-null; lane 3, *ARF/Mel18*-null; lane 4, *p53/Mel18*-null MEFs. (c-1) *ARF*-null (square) and *ARF/Mel18*-null (circle) MEFs (passage-7) were infected with mock virus (closed) or ARF virus (open), and then diluted to 2×10^4 per 60-mm diameter dish and replica plated. Individual cultures harvested every 2 days thereafter were counted. Values represent average and standard deviations of triplicate cultures. (c-2) *p53*-null (diamond) and *p53/Mel18*-null (triangle) MEFs (passage-7) were infected with mock virus (closed) or wild-type p53 virus (open). Cell proliferation analysis was then performed, as in Fig. 3c-1. Primer sequences for RT-PCR analysis are listed in Table 1.

Collinear decrease of Ring1b and E2F3b binding to the E2F site upon synergic effects of culture stress and Mel18 deficiency

We went on to examine the impact of replicative stress and Mel18 deficiency on Ring1b binding at the E2F binding site in the *ARF* promoter, 1st exon of *p19^{ARF}* (1st exon) and *p16^{INK4a}* promoter (Fig. 5a). Although all these regions bound Ring1b, the functional E2F site was

only seen to bind to the *ARF* promoter. Wild-type and *Mel18*-null MEFs cultured according to the modified 3T9 protocol were subjected to ChIP assays. Both wild-type and *Mel18*-null MEFs showed growth retardation at passage-6 in the modified 3T9 assay. In particular, proliferation ability was apparently impaired in *Mel18*-null MEFs (Fig. 1a,b). In wild-type MEFs, Ring1b association in these three regions was decreased in passage-6 MEFs compared with passage-2. In *Mel18*-null MEFs,
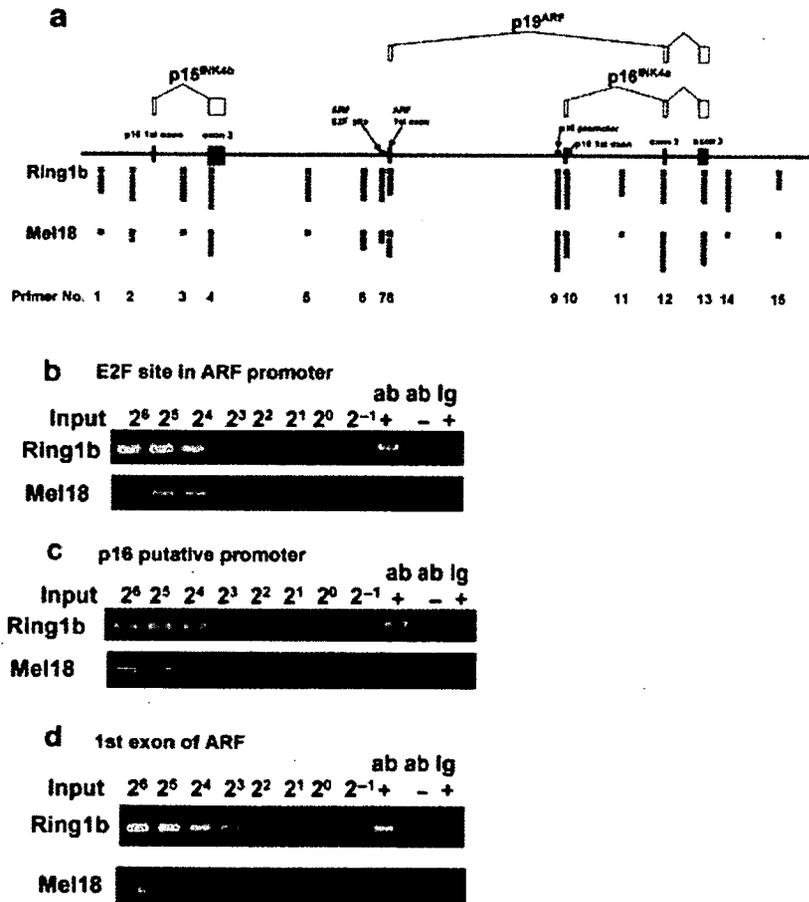
Figure 4 Analysis of the *in vivo* binding of polycomb proteins in the *INK4/ARF* region. (a) 11.5-dpc embryos were subjected to ChIP assays as described in Experimental procedures with anti-Ring1b mouse monoclonal antibody and anti-Mel18 goat serum. The squares represent the degree of enrichment of immunoprecipitated genomic DNA. Each square means twofold enrichment in comparison with un-fractionated 'input' DNA. (b–d) Representative results of three ChIP experiments which indicated the association of these polycomb proteins with the INK4/ARF locus: E2F site (b), *p16* promoter (c) and p19ARF exon 1 (d). 'Ig' means species-matched immunoglobulin as a negative control for immunoprecipitation (for Ring1b: mouse Ig, for Mel18: goat Ig).

Ring1b association was more strongly decreased than in the wild-type, which was highest in the region including an E2F site in comparison with the 1st exon of *ARF* (1st exon) and *p16^{INK4a}* promoter; therefore, Ring1b binding to the region including an E2F site was synergistically impaired by culture stress and Mel18 deficiency, although a weak association of Mel18 with this region in 11.5 dpc embryos was observed (Fig. 4b). We thus re-examined Mel18 association with the E2F site using MEFs (Fig. 5b). We found Mel18 association with the *p16* promoter but to neither the E2F site nor the 1st exonic region of the *ARF* gene. *Mel18*-null MEFs provided negative controls for this experiment; therefore, although Mel18 itself does not directly bind to the genomic region around the E2F site of the *ARF* promoter, Mel18 seems to regulate the binding of class II PcG complexes to the p15^{INK4b}/p19^{ARF}/p16^{INK4a} genomic locus by forming a complex with at least Ring1b.

The reduction of Ring1b binding to the E2F site in *Mel18*-null MEFs prompted us to examine E2F3b association with this region since E2F3b has been shown to

act as a repressor of *ARF* transcription (Aslanian *et al.* 2004). Since a specific antibody against E2F3b is not yet available to the best of our knowledge, we used antibodies that recognize E2F3a+b or E2F3a for ChIP assays and estimated E2F3b binding based on the differences of these two antibodies. Binding of E2F3a+b was seen at the E2F site and the 1st exonic region in 11.5 dpc embryos and passage-1 MEFs, but not at the *p16* promoter, irrespective of *Mel18* genotype (Fig. 5c), which is consistent with a previous report (Aslanian *et al.* 2004). A significant difference was seen in passage-2 MEFs between wild-type and *Mel18* mutants in that E2F3a+b binding was exclusively seen in the wild-type. In passage-6 MEFs, E2F3a+b binding was seen in neither wild-type nor *Mel18* mutants. E2F3a binding to the E2F site and 1st exonic region of *ARF* was seen in 11.5 dpc embryos, but not in MEFs (Fig. 5d), suggesting that the signals obtained by the anti-E2F3a+b antibody were derived from E2F3b. E2F3b may bind to the E2F site and 1st exonic region in MEFs and be exfoliated upon culture stress, which is exaggerated by Mel18 deficiency.
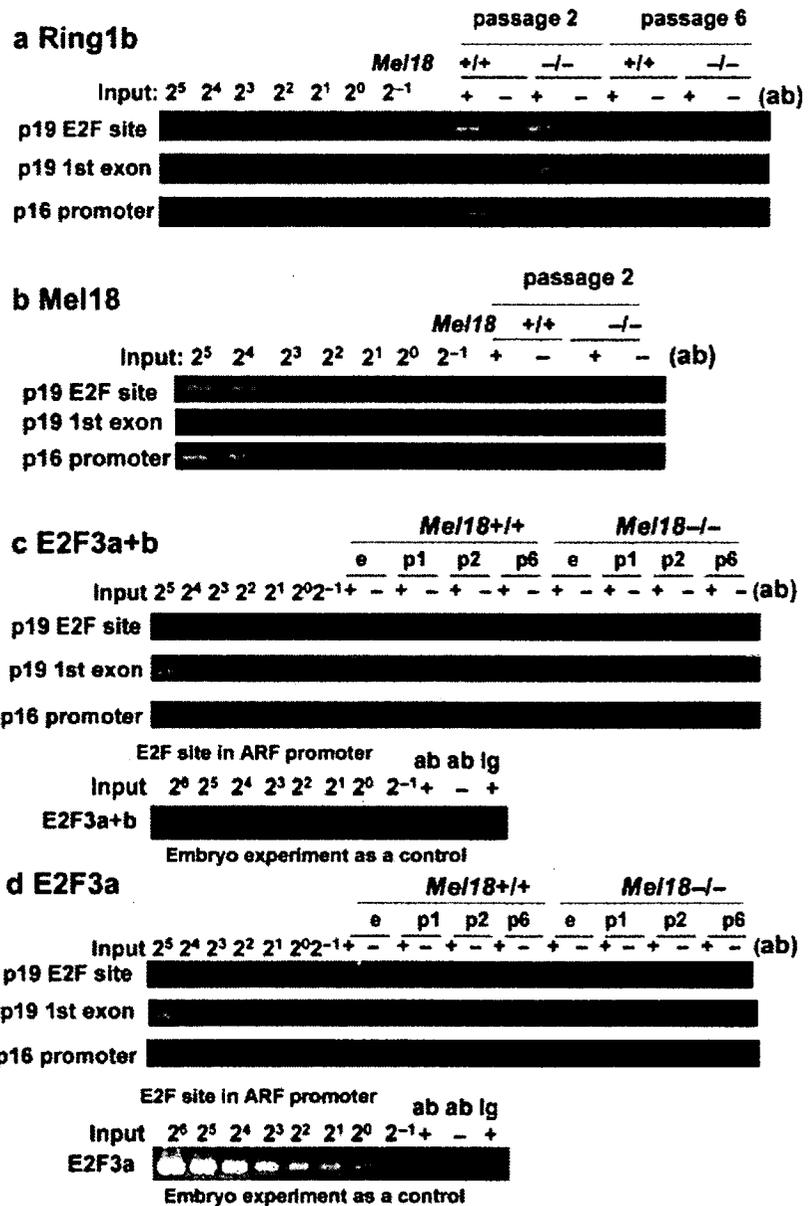
218

Figure 5 *In vivo* binding of polycomb proteins and E2F3s are attenuated in *Mel18*-null MEFs. MEFs derived from *Mel18*-null embryo and wild-type litter-mates were cultured by the modified 3T9 protocol and the passaged cells were analyzed by ChIP assays with the indicated antibodies (a, anti-Ring1b; b, anti-Mel18 goat serum; c, anti-E2F3a carboxyl terminus rabbit serum, which recognizes both E2F3a and E2F3b; d, anti-E2F3a amino terminus rabbit serum). Purified DNA was analyzed by PCR with primers specific for the E2F site and exon 1 for ARF and the p16 promoter region, as described in Experimental procedures. These are representative results of at least three independent experiments using different embryos. In (c) and (d), 'e',11.5 dpc-embryo; 'p1', passage-1; 'p2', passage-2; 'p6', passage-6. For E2F3a (d) and E2F3a+b (c) antibodies, experiments including rabbit immunoglobulin (Ig) were presented as negative controls.

Together, this implies that E2F3b and Ring1b binding to the E2F site are collinearly decreased upon culture stress and Mel18 deficiency. It is also noteworthy that culture stress was suggested to alter the balance of E2F3a and E2F3b at the E2F site and 1st exonic region.

PcG proteins and E2F3s form binary complexes

The above-mentioned results of ChIP assays, which indicate that Ring1b and E2F3b bind to the E2F site in the *ARF* promoter, prompted us to study whether PcG complexes can form binary complexes with E2F3b. We examined Mel18/E2F3s interaction in whole-cell extracts from 11.5 dpc embryos in which PcG complexes have been shown to act as repressors of *Hox* gene expression (Akasaka *et al.* 1996) and from passage-5 MEFs (Fig. 6). In 11.5 dpc embryos, significant amounts of Mel18 were immunoprecipitated by both anti-E2F3a and -E2F3a+b, although the signal given by anti-E2F3a+b was stronger than that by anti-E2F3a (Fig. 6a); however, Mel18 bound only to E2F3b and not to E2F3a in passage-5 MEFs (Fig. 6b). These observations are consistent with the results
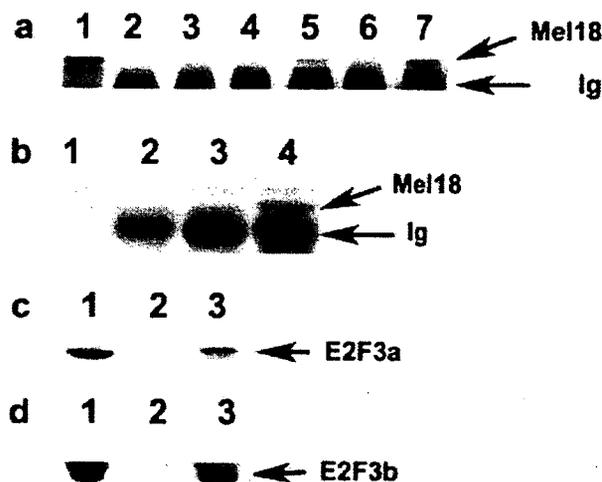
Figure 6 Polycomb proteins bind to E2F3s in embryos and MEFs. In Fig. 6a, lysate of a wild-type mouse embryo at 11.5 dpc (500 μg protein) was immunoprecipitated with goat immunoglobulin (lanes 2, 4 and 6) or Mel18 antibody (lanes 3, 5 and 7). In Fig. 6b–d, lysate from wild-type MEFs at passage-5 was analyzed. Western blot analysis was performed using Mel18 antibody (Fig. 6a,b) and E2F3a+b antibody (Fig. 6c,d). In lane 1, 20 μg protein of total cell lysate was analyzed as a control. Equal amounts of total cell lysates (500 μg protein) were subjected to IP with control IgG (lane 2), anti-E2F3a ab (b, lane 3), anti-E2F3a+b ab (b, lane 4), and anti-Ring1b ab (c and d, lane 3). In panels c and d, E2F3a and E2F3b were discriminated by their differences in relative molecular weights and by blotting with anti-E2F3a ab.

of ChIP assays that the E2F3a+b binding to p19 genomic regions seen in 11.5 dpc embryos rapidly disappeared after cells were explanted into culture (Fig. 5c,d). Meanwhile, Ring1b was shown to form complexes with both E2F3a and E2F3b in passage-5 MEFs (Fig. 6c,d). This may imply that PcG proteins interact with E2F3a outside INK4/ARF genomic regions in MEFs. These results suggest the presence of PcG/E2F3s binary complexes, and that the role of E2F3b in the transcriptional regulation of ARF may involve direct interactions with PcG complexes.

Discussion

In the present study, we first demonstrated that deficiency of the Mel18 component of class II PcG complexes results in premature senescence via de-repression of ARF expression and subsequent stabilization of p53, as well as Bmi1, M33, Phc1 and Phc2 components. ChIP analyses indicated that transcriptional repression of $p16^{INK4}/ARF$ by PcG gene products may involve direct interactions

between PcG complexes and genomic regions. This is consistent with another observation that the reduction of Ring1b binding at the ARF promoter in MEFs is correlated with the degree of premature senescence of MEFs, which is exaggerated by Mel18 deficiency, although it is possible that the accelerated exfoliation of PcGs was caused by enhanced senescence. Since genetic depletion of Mel18, Bmi1, M33, Phc1 or Phc2 uniformly exhibits premature senescence of MEFs accompanied by de-repression of ARF, all components of the class II complex may be indispensable to maintain fully functional PcG complexes at the ARF promoter under replicative stress. We thus postulate that the quantity of class II PcG complexes physically associated with the INK4/ARF region may be involved in limiting the transcriptional status of ARF and $p16^{INK4a}$. The molecular mechanisms regulating the quantity of class II PcG complexes are not known yet, although intrinsic mechanisms could at least be involved in maintaining the stability of complexes as manifested by mutant phenotypes of respective components, for example, the decrease of class II PcGs in Mel18-null MEFs (Fig. 2c). Moreover, Ring1b and Bmi1 components of class II PcG components have been shown to be linked to mono- and poly-ubiquitinylation of their targets (Wang et al. 2004; Cao et al. 2005; Hernandez-Munoz et al. 2005). These observations suggest that replicative stress is at least partly mediated by the binding of class II PcG complexes to the INK4/ARF region, and that ARF in particular regulates cellular senescence in MEFs.

It is noteworthy that although Mel18 deficiency impacted ARF transcription, no significant association of Mel18 with the ARF promoter region was observed in wild-type MEFs, but was seen in $p16^{INK4a}$-promoter and exonic regions (Fig. 4,5). This again implies that Mel18 mediates transcriptional regulation of the INK4/ARF region by forming multimeric protein complexes, in which the Mel18 component may not be juxtaposed to ARF-promoter/1st exon regions. Another possibility involves other multimeric complexes, including Ring1b, but not Mel18, which bind to ARF-specific regions, such as E2F6 complexes (Ogawa et al. 2002). This latter possibility is supported by our unpublished observation that mutant allele products of the MBLR gene, which are components of E2F6 complexes and interact with Ring1b, exhibit genetic interactions with Mel18 mutations, at least at Hox cluster loci (J. Shinga and H.K., unpubl. obs.). The binding of the E2F6 complex components and mutant interactions between Mel18 and MBLR genes in the INK4/ARF region should be addressed in future.

Similarly to Ring1b binding, the association of E2F3b, which is also essential for transcriptional repression of ARF, with the ARF promoter region was correlated with the

degree of cellular senescence of MEFs. Moreover, associations of E2F3b and Ring1b with the *ARF* promoter were collinearly decreased with synergistic effects of culture stress and Mel18 deficiency. E2F3b and Ring1b are capable of interacting directly upon mammalian cells (Fig. 6). This implies that the association of E2F3b with the *ARF* promoter may be at least partly dependent on class II PcG complexes at that locus. The convergence of class II complexes and E2F3b at the *ARF* promoter may be required to repress *ARF* transcription in MEFs, and binary complexes are presumably exfoliated by the stress that cells experience when explanted into culture.

Intriguingly, although significant binding of E2F3b or E2F3a was not seen at the $p16^{INK4a}$ promoter, $p16^{INK4a}$ has been shown to be de-repressed in *E2F3a+b* -null MEFs, as well as ARF (Aslanian *et al.* 2004). This implies that repression of the $p16^{INK4a}$ promoter is also impacted by E2F3s, which may bind to the *ARF* promoter and/ or 1st exonic regions. Since the $p16^{INK4a}$ promoter is bound by class II PcG complexes, class II complexes may require E2F3s for repressive functions at the $p16^{INK4a}$ locus in MEFs. From these results, we can surmise that class II PcG complexes and E2F3s act in mutually dependent manners in the *INK4/ARF* region. The formation of binary complexes may mediate various signals to the locus, since both oncogenic signals and culture stress were shown to alter the binding of E2F3s to the E2F site of the *ARF* promoter. It will be important to further address the binding of class II PcG components to the *INK4/ARF* region of *E2F3a+b* -null MEFs.

Moreover, it is notable that E2F3b bound to the *ARF* promoter/1st exon irrespective of the E2F site, which is required to mediate transcriptional regulation by E2F family proteins. Since E2F3b is capable of interacting with Ring1b, it is possible that the binding of E2F3b to the first exonic region of ARF is mediated by its interaction with class II PcG complexes rather than with genomic components. It may also be true that there are some discriminating activities to recruit E2F3b between *ARF*- and $p16^{INK4a}$-genomic regions, although both are bound by Ring1b. Since *ARF* and $p16^{INK4a}$ genomic regions are quite different in terms of Mel18 binding in MEFs, it is possible that different interactions for Ring1b in respective regions could play a role. We thus suggest that class II PcG complexes and E2F3b interact in the *INK4/ARF* region and mutually regulate each other's function to limit cellular senescence.

It is notable that another E2F family protein, E2F6, is reported to interact with PcG and its related complexes, which exert a significant impact on the transcription of cell cycle-related genes (Trimarchi *et al.* 2001; Ogawa *et al.* 2002); however, E2F6 is only distantly related to

other E2Fs and lacks the sequences responsible for both transactivation and binding to retinoblastoma protein. In support of this, E2F6-deficient mouse experiments indicate that E2F6 is essential for the long-term somatic silencing of certain male germ-cell-specific genes, but it is dispensable for cell-cycle regulation (Pohlers *et al.* 2005). Meanwhile, *E2F3a/E2F3b* double-null MEFs showed severe retardation in cell cycle progression (Aslanian *et al.* 2004) and our present study indicates that class II PcGs and E3F3s act in a mutually dependent manner in the regulation of $p16^{INK4a}$/*ARF* transcription. Taken together, it is possible that, in concert with PcG proteins, different E2F family proteins may be utilized to mediate transcriptional regulation in a locus- or cell type-specific manner.

We are currently planning to study the impact of oncogenic stresses, for example, Myc and E2Fs, on the binding of class II PcG proteins and E2F3s via the E2F site, 1st exon of ARF and p16 promoter regions. This will be informative to address the role of PcGs and E2F3s in tumor suppression by the control of stress-induced cellular arrest or apoptotic cell death induced by oncogene products via ARF/p16[INK4a].

Experimental procedures

Reagents and antibodies

Anti-p21[Cip1/Waf1] mouse monoclonal antibody (clone F-5), anti-E2F3a rabbit serum (antibody against N-terminal of E2F3a: sc-879) and anti-E2F3a+b rabbit serum (antibody against common C-terminal of E2F3a and E2F3b: sc-878) were from Santa Cruz Biotechnology, Inc. (Santa Cruz, CA). Anti-p19[ARF] rabbit polyclonal antibody (R562) and anti-Mel18 goat serum (ab5267) were purchased from Abcam (Cambridge, UK). Anti-HA antibody (clone 12CA5) and anti-β-tubulin mouse monoclonal antibody were purchased from Boehringer Mannheim K.K. (Tokyo, Japan). Anti-p53 mouse monoclonal antibody (clone pAb421) was from Oncogene Research Products (Cambridge, MA). Anti-mouse p16 monoclonal antibody (16P04) was from NeoMarkers (Fremont, CA). Anti-MDM2 mouse monoclonal antibody (clone 2A10) was kindly provided by Dr A.J. Levine. Anti-Ring1b mouse monoclonal antibodies were as described in a previous report (Isono *et al.* 2005). Anti-Bmi1 antibody (clone 229F6) was from Upstate (Lake Placid, NY). Other biochemical reagents were purchased from Sigma-Aldrich Japan (Tokyo, Japan), or Wako (Osaka, Japan).

Interbreeding of mice

The generation of *Mel18*-null (Akasaka *et al.* 1996), *ARF*-null (Kamijo *et al.* 1997) and *p53*-null (Gondo *et al.* 1994), each with a 129/svj × C57BL/6 background, was described in previous reports. These mice had been backcrossed to a C57BL/6 background more than 8 times, and were interbred to yield animals lacking Mel18/p53 or Mel18/ARF.

Table 1 Primer sequences used in RT-PCR experiments

Gene	Forward primer sequence	Reverse primer sequence	Accession number
p19ARF	agggatccttggtcactgtgaggattc	gcaaagcttgaggccggatttagctctgctc	BC058190
p16INK4a	cgggatccgctgcagacagactggccag	gcaaagcttgaggccggatttagctctgctc	L76150
Mel18	ccaccaccattgtggaatgc	tcccgt7gccgtttcatttc	BC016419
Bmi1	tacttggagaccagcaagta	cctcttctcctcatctgcaa	NM_007552
Ring1b	gtgaattaatgtgcccaatt	ctttcctgatgcgcttcata	BC020122
G3PDH	accacagtccatgccatcac	tccaccaccctgttgctgta	NM_002046

Cells and cell culture

MEFs were prepared as described previously (Kamijo *et al.* 1997). *Mel18*-null, *Mel18/ARF* and *Mel18/p53* double-null MEFs were routinely maintained with DMEM supplemented with 20% fetal bovine serum (FBS), 1× non-essential amino acid (GibcoBRL[®]) and 1× penicillin–streptomycin (GibcoBRL[®]).

To induce senescence effectively, 3 × 10⁶ cells were plated in a 10-cm diameter dish, passaged at 3-day intervals, counted after trypsinization, and the number of cells per dish was recorded. One-third of cells were re-plated in a 10-cm diameter dish every 3 days (Fig. 1a).

In modified 3T9 assays, cells were passaged at 3-day intervals and counted after trypsinization, and the number of cells per dish was recorded. Amounts of 1 × 10⁶ cells were re-plated in 60-mm diameter dishes every 3 days (Fig. 3a; Kamijo *et al.* 1997). In growth-speed assays, cells diluted at 2 × 10⁴ per 60-mm diameter dish were replica plated, and individual cultures harvested every day thereafter were counted (Figs 1b and 3c).

Procedure for senescence-associated β-galactosidase staining of MEFs

In situ SA-β-Gal activity was detected according to the manufacturer's protocol (Senescence Detection Kit, BioVision, Mountain View, CA). Briefly, MEFs were washed with PBS, fixed with fixation solution for 15 min at room temperature, washed twice with PBS and stained for 16 h at 37 °C with 1 mg/mL 5-bromo-4-chloro-3-indolyl-β-galactoside (X-Gal) staining solution. Micrographs of β-galactosidase-stained MEFs were taken at 400× magnification using a phase contrast microscope (Olympus, Japan).

Apoptosis assay

Sub-G0/G1 fractions were analyzed using a FACScan flow cytometer (Becton Dickinson, San Jose, CA). Samples of 15 000 cells were analyzed for each sample, and quantitation of cell-cycle distribution was performed using Cell Quest software (Becton Dickinson).

Retrovirus production and infection

A retrovirus vector for virus production, pMSCV-IRES-GFP, was a generous gift from Dr Robert G. Hawley, The George Washington University Medical Center. Virus production and cell infection were performed using retroviral helper and vector plasmids provided by Charles Sawyers (University of California, Los Angeles, CA). Cells from the human kidney 293T cell line were from Dr David Baltimore (California Institute of Technology, Pasadena, CA). The following cDNAs were cloned into pMSCV-IRES-GFP or pSRa-MSV-tk-CD8 plasmids for production of recombinant retroviruses expressing wild-type p53 and ARF. Wild-type *p53* and mouse *ARF* cDNAs were provided by Drs C.J. Sherr and M.F. Roussel, St. Jude Children's Research Hospital. For virus infection of MEFs, three infections at 4-h intervals with high-titer replication-defective viruses were performed. Virus infection efficiency was determined 48 h after infection by fluorescence-activated flow cytometry (FACS) as a percentage of GFP-positive cells compared to non-infected cells.

Analysis of RNA and protein expression

Immunoprecipitation and Western blotting were performed according to previous reports (Kamijo *et al.* 1998; Nakazawa *et al.* 2003). Total RNA was extracted from NB cells using Isogen[®] (Wako, Tokyo, Japan), and cDNA was synthesized from 1 µg of total RNA templates according to the manufacturer's protocol (RiverTra-Ace-α- RT-PCR kit, TOYOBO, Osaka, Japan). PCR amplification was performed using the primers listed in Table 1. Semi-quantitative RT-PCR analysis was performed according to the previous report (Machida *et al.* 2006).

Chromatin-immunoprecipitated (ChIP) assay

ChIP assay was performed as described previously (Fujimura *et al.* 2006). Briefly, either minced embryos or MEFs were chemically cross-linked in 1% formaldehyde–PBS for 10 min. After washing 3 times with PBS and once with TE (Tris–EDTA pH 8.0), tissues were suspended in a ten fold volume of TE. To solubilize proteins and cleave genomic DNA to average 2 kbp, samples were subjected to repeated sonication and ice-chilling. Insoluble matter was removed by centrifugation at 20 400 *g* for 5 min. Correct amounts of NaCl and NP-40 were added to the supernatants in order to perform optimal immunoprecipitation for each antibody (100 mM NaCl and 0.4% NP-40 for anti-Ring1b, 200 mM NaCl, and 0.1% NP-40 for anti-Mel18, anti-E2F3a and anti-E2F3a+b). Precleared protein extracts were incubated with the correct amount of antibodies, at 4 °C with rocking, from 2 h to overnight. Immune complexes were captured through 3-h incubation with Protein A Sepharose beads.

Table 2 Primer sequences used in Fig. 4

No.	F	R	Description
1	atgacgtcagcacttgctgg	tacaccgactattgactatg	2.2 kbp upstream from 1st exon of p15
2	aatagccaaccggccacggt	cgctcgagcgctagcgcctg	0.5 kbp upstream from 1st exon of p15
3	gatacagaacccacagccag	agtgcaggttagaggtgtag	Intronic region of p15
4	cagtcatgatgatgggcag	tctccagtggcagcgtgcag	2nd exon of p15
5	agggtaggctccatgagaag	tccataatctttgctcaaga	Intermediate region between p15 2nd exon and p19 1st exon
6	cttcctatgtctagtactgg	gccatccgtctggactagtt	Intermediate region between p15 2nd exon and p19 1st exon
7	gctggctgtcaccgcgat	gcgttgaggcacctcgaga	E2F site in p19 promoter
8	ctcacctcgcttgtcacagt	tcctacctggtccaggattc	p19 1st exon
9	tcgagaaggactagttcact	ttgccctgaatatagcatga	p16 promoter
10	cgaactcgaggagagccatc	acactccttgcctacctgaa	p16 1st exon
11	acctgcagagccatcttgca	aatacatgtgctgaagatat	1st intronic region of p16
12	tcacgtagcagctcttctgc	cagcggaacgcaaatatcgc	2nd exon of p16/p19
13	cacctaggacagctttatat	tctgctccctccccgtgattgc	3rd exon of p19/p19
14	agagaaggctcacagaagca	tagtgacgtgctgtaagaga	0.5 kbp down stream from 3rd exon of p16/p19
15	gatctttcacatatatgtac	tgattgctcttctgaaggtc	5.3 kbp down stream from 3rd exon of p16/p19

Primer numbers are mentioned in Fig. 4a.

Beads were washed with the same components as immunoprecipitation 3 times briefly and 7 times for 10 min under intense rotation.

To isolate genomic DNA from immune complexes, beads were treated with 50 µg/mL of RNaseA at 37 °C for 30 min followed by overnight incubation with 500 µg/mL Proteinase K/0.5% SDS at 37 °C. After 3-h heating at 65 °C for reverse cross-linking, supernatants were collected, extracted by phenol–chloroform and concentrated by ethanol precipitation. Genomic DNA was also isolated from the original lysates through the same procedure as described above and designated as 'Input' DNA in Figs 4 and 5. To measure the DNA yield after immunoprecipitation, aliquots of immunoprecipitated DNA were electrophoresed for 5 min in an agarose gel, and then serially diluted input DNA and band intensities were compared after ethidium bromide staining.

An equivalent amount of immunoprecipitated DNA to that of 'Input' DNA loaded in lane '2^n' was subjected to PCR reactions. Usually 10–20 ng of genomic DNA was used. Mock-immunoprecipitated DNA (ab-) and species-matched immunoglobulin-immunoprecipitated DNA (Ig), derived from the same volume of the chromatin fraction used for specific antibody immunoprecipitation, were subjected to PCR. To carry out semi-quantitative PCR, serially diluted 'Input' DNA and immunoprecipitated DNA were used as templates. The relative quantity of each genomic region in immunoprecipitated genomic DNA was estimated by referring to serial dilutions of 'Input' DNA isolated from the initial lysates and an enrichment value was determined. Each series of experiments was performed at least 3 times. Primers used in this study are listed in Table 2.

References

Akasaka, T., Kanno, M., Balling, R., Mieza, M.A., Taniguchi, M. & Koseki, H. (1996) A role for mel-18, a Polycomb group-related vertebrate gene, during theanteroposterior specification of the axial skeleton. *Development* **122**, 1513–1522.

Aslanian, A., Iaquinta, P.J., Verona, R. & Lees, J.A. (2004) Repression of the Arf tumor suppressor by E2F3 is required for normal cell cycle kinetics. *Genes Dev.* **23**, 1413–1422.

Cao, R., Tsukada, Y. & Zhang Y. (2005) Role of Bmi-1 and Ring1A in H2A ubiquitylation and Hox gene silencing. *Mol. Cell* **20**, 845–854.

Core, N., Bel, S., Gaunt, S.J., Aurrand-Lions, M., Pearce, J., Fisher, A. & Djabali, M. (1997) Altered cellular proliferation and mesoderm patterning in Polycomb-M33-deficient mice. *Development* **124**, 721–729.

Core, N., Joly, F., Boned, A. & Djabali, M. (2004) Disruption of E2F signaling suppresses the INK4a-induced proliferative defect in M33-deficient mice. *Oncogene* **23**, 7660–7668.

Fujimura, Y., Isono, K., Vidal, M., Endoh, M., Kajita, H., Mizutani-Koseki, Y., Takihara, Y., van Lohuizen, M., Otte, A., Jenuwein, T., Deschamps, J. & Koseki, H. (2006) Distinct roles of Polycomb group gene products in transcriptionally repressed and active domains of Hoxb8. *Development* **133**, 2371–2381.

Gondo, Y., Nakamura, K., Nakao, K., Sasaoka, T., Ito, K., Kimura, M. & Katsuki, M. (1994) Gene replacement of the p53 gene with the lacZ gene in mouse embryonic stem cells and mice by using two steps of homologous recombination. *Biochem. Biophys. Res. Commun.* **202**, 830–837.

Hernandez-Munoz, I., Lund, A.H., van der Stoop, P., Boutsma, E., Muijrers, I., Verhoeven, E., Nusinow, D.A., Panning, B., Marahrens, Y. & van Lohuizen. M. (2005) Stable X chromosome inactivation involves the PRC1 Polycomb complex and requires histone MACROH2A1 and the CULLIN3/SPOP ubiquitin E3 ligase. *Proc. Natl. Acad. Sci. USA* **102**, 7635–7640.

Humbert, P.O., Verona, R., Trimarchi, J.M., Rogers, C., Dandapani, S. & Lees, J.A. (1998) E2f3 is critical for normal cellular proliferation. *Genes Dev.* **12**, 690–703.

Isono, K., Fujimura, Y., Shinga, J., Yamaki, M., O-Wang, J., Takihara, Y., Murahashi, Y., Takada, Y., Mizutani-Koseki, Y. & Koseki, H. (2005) Mammalian polyhomeotic homologues Phc2 and Phc1 act in synergy to mediate polycomb repression of Hox genes. *Mol. Cell. Biol.* **25**, 6694–6706.

Itahana, K., Zou, Y., Itahana, Y., Martinez, J.L., Beausejour, C., Jacobs, J.J., Van Lohuizen, M., Band, V., Campisi, J. & Dimri, G.P. (2003) Control of the replicative life span of human fibroblasts by p16 and the polycomb protein Bmi-1. *Mol. Cell. Biol.* **23**, 389–401.

Iwama, A., Oguro, H., Negishi, M., Kato, Y., Morita, Y., Tsukui, H., Ema, H., Kamijo, T., Katoh-Fukui, Y., Koseki, H., van Lohuizen, M. & Nakauchi, H. (2004) Enhanced self-renewal of hematopoietic stem cells mediated by the polycomb gene product Bmi-1. *Immunity* **21**, 843–851.

Jacobs, J.J. & van Lohuizen, M. (2002) Polycomb repression: from cellular memory to cellular proliferation and cancer. *Biochim. Biophys. Acta* **1602**, 151–161.

Jacobs, J.J., Kieboom, K., Marino, S., DePinho, R.A. & van Lohuizen, M. (1999) The oncogene and Polycomb-group gene bmi-1 regulates cell proliferation and senescence through the ink4a locus. *Nature* **397**, 164–168.

Kamijo, T., Weber, J.D., Zambetti, G., Zindy, F., Roussel, M.F. & Sherr, C.J. (1998) Functional and physical interactions of the ARF tumor suppressor with p53 and Mdm2. *Proc. Natl. Acad. Sci. USA* **95**, 8292–8297.

Kamijo, T., Zindy, F., Roussel, M.F., Quelle, D.E., Downing, J.R., Ashmun, R.A., Grosveld, G. & Sherr, C.J. (1997) Tumor suppression at the mouse INK4a locus mediated by the alternative reading frame product p19ARF. *Cell* **91**, 649–659.

Kanno, M., Hasegawa, M., Ishida, A., Isono, K. & Taniguchi, M. (1995) mel-18, a Polycomb group-related mammalian gene, encodes a transcriptional negative regulator with tumor suppressive activity. *EMBO J.* **14**, 5672–5678.

Leone, G., DeGregori. J., Yan. Z., Jakoi. L., Ishida, S., Williams, R.S. & Nevins, J.R. (1998) E2F3 activity is regulated during the cell cycle and is required for the induction of S phase. *Genes Dev.* **12**, 2120–2130.

Lessard, J., Schumacher, A., Thorsteinsdottir, U., van Lohuizen, M., Magnuson, T. & Sauvageau, G. (1999) Functional antagonism of the Polycomb-Group genes eed and Bmi1 in hemopoietic cell proliferation. *Genes Dev.* **13**, 2691–2703.

Levine, S.S., King, I.F. & Kingston, R.E. (2004) Division of labor in polycomb group repression. *Trends Biochem. Sci.* **29**, 478–485.

Machida, T., Fujita, T., Ooo, M.L., Ohira, M., Isogai, E., Mihara, M., Hirato, J., Tomotsune, D., Hirata, T., Fujimori, M., Adachi, W. & Nakagawara, A. (2006) Increased expression of proapoptotic BMCC1, a novel gene with the BNIP2 and Cdc42GAP homology (BCH) domain, is associated with favorable prognosis in human neuroblastomas. *Oncogene* **25**, 1931–1942.

Nakazawa, Y., Kamijo, T., Koike, K. & Noda, T. (2003) ARF tumor suppressor induces mitochondria-dependent apoptosis by modulation of mitochondrial Bcl-2 family proteins. *J. Biol. Chem.* **278**, 27888–27895.

Ogawa, H., Ishiguro, K., Gaubatz, S., Livingston, D.M. & Nakatani, Y. (2002) A complex with chromatin modifiers that occupies E2F- and Myc-responsive genes in G0 cells. *Science* **296**, 1132–1136.

Ohta, H., Sawada, A., Kim, J.Y., Tokimasa, S., Nishiguchi, S., Humphries, R.K., Hara, J. & Takihara, Y. (2002) Polycomb group gene rae28 is required for sustaining activity of hematopoietic stem cells. *J. Exp. Med.* **195**, 759–770.

Park, I.K., Qian, D., Kiel, M., Becker, M.W., Pihalja, M., Weissman, I.L., Morrison, S.J. & Clarke, M.F. (2003) Bmi-1 is required for maintenance of adult self-renewing haematopoietic stem cells. *Nature* **423**, 302–305.

Pohlers, M., Truss, M., Frede, U., Scholz, A., Strehle, M., Kuban, R.J., Hoffmann, B., Morkel, M., Birchmeier, C. & Hagemeier, C. (2005) A role for E2F6 in the restriction of male-germ-cell-specific gene expression. *Curr. Biol.* **15**, 1051–1057.

Sears, R.C. & Nevins, J.R. (2002) Signaling networks that link cell proliferation and cell fate. *J. Biol. Chem.* **277**, 11617–11620.

Sherr, C.J. & DePinho, R.A. (2000) Cellular senescence: mitotic clock or culture shock? *Cell* **102**, 407–410.

Suzuki, M., Mizutani-Koseki, Y., Fujimura, Y., Miyagishima, H., Kaneko, T., Takada, Y., Akasaka, T., Tanzawa, H., Takihara, Y., Nakano, M., Masumoto, H., Vidal, M., Isono, K. & Koseki, H. (2002) Involvement of the Polycomb-group gene Ring1B in the specification of the anterior-posterior axis in mice. *Development* **129**, 4171–4183.

Trimarchi, J.M., Fairchild, B., Wen, J. & Lees, J.A. (2001) The E2F6 transcription factor is a component of the mammalian Bmi1-containing polycomb complex. *Proc. Natl. Acad. Sci. USA* **98**, 1519–1524.

van der Lugt, N.M., Domen, J., Linders, K., van Roon, M., Robanus-Maandag, E., te Riele, H., van der Valk, M., Deschamps, J., Sofroniew, M., van Lohuizen, M. & Berns, A. (1994) Posterior transformation, neurological abnormalities, and severe hematopoietic defects in mice with a targeted deletion of the bmi-1 proto-oncogene. *Genes Dev.* **8**, 757–769.

Wang, H., Wang, L., Erdjument-Bromage, H., Vidal, M., Tempst, P., Jones, R.S. & Zhang, Y. (2004) Role of histone H2A ubiquitination in Polycomb silencing. *Nature* **431**, 873–878.

Zindy, F., Eischen, C.M., Randle, D.H., Kamijo, T., Cleveland, J.L., Sherr, C.J. & Roussel, M.F. (1998) Myc signaling via the ARF tumor suppressor regulates p53-dependent apoptosis and immortalization. *Genes Dev.* **12**, 2424–2433.

Novel regulation of MHC class II function in B cells

Yohei Matsuki[1,9], Mari Ohmura-Hoshino[1,9], Eiji Goto[1], Masami Aoki[1], Mari Mito-Yoshida[1], Mika Uematsu[1], Takanori Hasegawa[2], Haruhiko Koseki[2], Osamu Ohara[3,4], Manabu Nakayama[4], Kiminori Toyooka[5], Ken Matsuoka[5,6], Hak Hotta[7], Akitsugu Yamamoto[8] and Satoshi Ishido[1,]*

[1]Laboratory for Infectious Immunity, RIKEN Research Center for Allergy and Immunology, Tsurumi-ku, Yokohama, Kanagawa, Japan, [2]Laboratory for Developmental Genetics, RIKEN Research Center for Allergy and Immunology, Tsurumi-ku, Yokohama, Kanagawa, Japan, [3]Laboratory for Immunogenomics, RIKEN Research Center for Allergy and Immunology, Tsurumi-ku, Yokohama, Kanagawa, Japan, [4]Kazusa DNA Research Institute, Kisarazu, Chiba, Japan, [5]RIKEN Plant Science Center, Tsurumi-ku, Yokohama, Kanagawa, Japan, [6]Laboratory of Plant Nutrition, Faculty of Agriculture, Kyushu University, Higashi-ku, Fukuoka, Japan, [7]Division of Microbiology, Department of Genome Sciences, Kobe University Graduate School of Medicine, Chuo-ku, Kobe, Hyogo, Japan and [8]Faculty of Bio-Science, Nagahama Institute of Bio-Science and Technology, Nagahama, Japan

The presence of post-translational regulation of MHC class II (MHC II) under physiological conditions has been demonstrated recently in dendritic cells (DCs) that potently function as antigen-presenting cells (APCs). Here, we report that MARCH-I, an E3 ubiquitin ligase, plays a pivotal role in the post-translational regulation of MHC II in B cells. MARCH-I expression was particularly high in B cells, and the forced expression of MARCH-I induced the ubiquitination of MHC II. In B cells from MARCH-I-deficient mice (MARCH-I KO), the half-life of surface MHC II was prolonged and the ubiquitinated form of MHC II completely disappeared. In addition, MARCH-I-deficient B cells highly expressed exogenous antigen-loaded MHC II on their surface and showed high ability to present exogenous antigens. These results suggest that the function of MHC II in B cells is regulated through ubiquitination by MARCH-I.

Introduction

Ubiquitination is an essential post-translational modification of proteins that 'marks' proteins with ubiquitin molecules,

*Corresponding authors. Laboratory for Infectious Immunity, RIKEN Research Center for Allergy and Immunology, 1-7-22 Suehiro-cho, Tsurumi-ku, Yokohama, Kanagawa 230-0045, Japan.
Tel.: +81 45 503 7022; Fax: +81 45 503 7021;
E-mail: ishido@rcai.riken.jp
[9]These authors equally contributed to this work

often resulting in degradation (Hershko and Ciechanover, 1998). This modification is achieved through the action of three enzymes: ubiquitin-activating enzyme E1 (E1), ubiquitin-conjugating enzyme E2 (E2), and ubiquitin-protein ligase E3 (E3). E1 activates ubiquitin, and the activated ubiquitin is subsequently transferred to a substrate through the interaction of E2 and E3. Whereas E2 carries the activated ubiquitin, E3 conjugates ubiquitin moieties to the target substrate (Hershko and Ciechanover, 1998).

At present, ubiquitination is thought to play an important role in the degradation of membrane proteins through the induction of endocytosis (Dupre et al, 2004). In yeast, an E3, Rsp5p, has been reported to induce ubiquitination of the cytoplasmic tail of substrate proteins, a step that is necessary for the endocytosis and degradation of the substrate proteins (Dupre et al, 2004). Similarly, we and other groups have recently identified a novel family of E3 enzymes termed MIR family, whose catalytic domain is a variant RING domain (RINGv domain). The MIR family members have been shown to induce rapid endocytosis and degradation through the ubiquitination of the cytoplasmic tail of substrate proteins in mammals (Coscoy et al, 2001; Coscoy and Ganem, 2003; Goto et al, 2003; Bartee et al, 2004; Lehner et al, 2005; Ohmura-Hoshino et al, 2006a). The MIR family proteins share a secondary structure and the RINGv domain located at the amino terminus. They bind to the membrane through their hydrophobic domains located at the center, and possess two intracellular regions.

Most importantly, the forced expression of MIR family members was found to be capable of degrading immune recognition-related molecules, such as MHC class I (MHC I) and MHC II (Coscoy and Ganem, 2000, 2001; Ishido et al, 2000a, b; Fruh et al, 2002; Ohmura-Hoshino et al, 2006b). However, the physiological substrates for these novel ubiquitin ligases remain completely unknown. Among the MIR family members, c-MIR and MARCH-I are of particular interest, because they can efficiently degrade important proteins in the immune system, and the surface expression of MHC II has been shown recently to be regulated by ubiquitination in dendritic cells (DCs) that potently function as antigen-presenting cells (APCs) (Goto et al, 2003; Bartee et al, 2004; Ohmura-Hoshino et al, 2006b; Shin et al, 2006). Within the E3 catalytic domain and transmembrane regions, the amino-acid identity between c-MIR and MARCH-I is >80%, suggesting similar functions. As MARCH-I expression was reported to be restricted to secondary lymphoid tissues such as spleen and lymph node, we have been especially interested in the functional elucidation of MARCH-I (Bartee et al, 2004).

In this report, we demonstrate that in B cells, the surface expression of MHC II is regulated through ubiquitination by MARCH-I, and the ubiquitination does not contribute to the internalization of surface MHC II. In parallel with the stabilization of surface MHC II, we found that MARCH-I-deficient B cells highly expressed exogenous antigen-loaded MHC II on their surface and showed high ability to present exogenous antigens. Thus, our results suggest that the function of MHC